AGU ADVANCING EARTH AND SPACE SCIENCE

Water Resources Research

REVIEW ARTICLE
10.1029/2022WR032219

Remote Sensing of Groundwater: Current Capabilities and Future Directions

Kyra H. Adams[1], John T. Reager[1], Paul Rosen[1], David N. Wiese[1], Tom G. Farr[1,†], Shanti Rao[1], Bruce J. Haines[1], Donald F. Argus[1], Zhen Liu[1], Ryan Smith[2], James S. Famiglietti[3], and Matthew Rodell[4]

[1]Jet Propulsion Laboratory, California Institute of Technology, Pasadena, CA, USA, [2]Department of Civil and Environmental Engineering, Colorado State University, Collins, CO, USA, [3]Global Institute for Water Security, University of Saskatchewan, Saskatoon, SK, Canada, [4]NASA Goddard Space Flight Center, Greenbelt, MD, USA

[†]Retired

Key Points:

- Accurately measuring and monitoring groundwater storage and fluxes is critical for water, food, and energy security
- Remote sensing approaches such as gravitational measurements, Interferometric Synthetic Aperture Radar, Global Navigational Satellite System, lidar altimetry, and Airborne Electromagnetic Systems can yield indirect yet valuable information about groundwater
- Fusing multiple remotely sensed data sets or employing other tools such as numerical models increase the applicability of individual approaches

Correspondence to:
J. T. Reager,
john.reager@jpl.nasa.gov

Citation:
Adams, K. H., Reager, J. T., Rosen, P., Wiese, D. N., Farr, T. G., Rao, S., et al. (2022). Remote sensing of groundwater: Current capabilities and future directions. *Water Resources Research*, *58*, e2022WR032219. https://doi.org/10.1029/2022WR032219

Received 21 MAR 2022
Accepted 16 SEP 2022

Author Contributions:
Visualization: Paul Rosen, David N. Wiese, Tom G. Farr, Bruce J. Haines, Donald F. Argus, Matthew Rodell
Writing – original draft: Paul Rosen, David N. Wiese, Tom G. Farr, Shanti Rao, Bruce J. Haines, Donald F. Argus
Writing – review & editing: Paul Rosen, David N. Wiese, Tom G. Farr, Shanti Rao, Bruce J. Haines, Donald F. Argus, Zhen Liu, James S. Famiglietti, Matthew Rodell

Abstract Globally, groundwater represents a critical natural resource that is affected by changes in natural supply and renewal, as well as by increasing human demand and consumption. However, despite its critical role, groundwater is difficult to accurately quantify as it is beneath the Earth surface. Here, we review several state-of-the-art remote sensing techniques useful for local- to global-scale groundwater monitoring and assessment, including proxies for groundwater extraction. These include inferring changes in subsurface water from mass changes using gravitational measurements, and analyzing changes in the Earth surface height using Interferometric Synthetic Aperture Radar, Light Detection and Ranging, Airborne Electromagnetic Systems, and satellite altimetry. Remote sensing information is often used in tandem with ground-based observations such as hydraulic head in wells, Global Navigational Satellite System monitoring, and numerical modeling to complement the space-based approaches. In the future, fusing different remote sensing techniques capable of operating in various environments will yield additional insight on the state and rate of use for groundwater across the globe.

1. Scientific Necessity and Overview

Groundwater is Earth's largest reservoir of fresh, liquid water. Accounting for more than 20% of water usage worldwide and 43% of irrigation water (Earman & Dettinger, 2011; Fetter, 2001; Zektser & Everett, 2004), groundwater serves as the primary source of freshwater for over 2 billion people across the globe (Alley et al., 2002; Famiglietti et al., 2011; Gleeson et al., 2012; WWAP, 2015). Its contributions are expected to increase with rising global population and changing climate, as surface water becomes a less reliable resource (FAO, 2005; OECD, 2011; WWAP, 2015). It is estimated that by 2050, 2 billion additional people will need to be fed, increasing demand on agricultural land use for improved rates of food production (OECD, 2011; WWAP, 2015). As climate change continues to alter patterns of drought and regional recharge dynamics, groundwater will continue to establish itself as an increasingly critical component of the water cycle, as groundwater variability directly impacts surface water (Döll, 2009; Earman & Dettinger, 2011; Maxwell & Kollet, 2008; Scibek & Allen, 2006). Groundwater also has important implications for the energy cycle, as it can act as a thermal energy storage (Arola et al., 2016; Dickinson et al., 2009) or an energy consumer during its abstraction (Kumar, 2005; Scott & Sharma, 2009; Wang et al., 2012). Groundwater supply, therefore, is directly linked to global food safety, climate change, and energy security (Famiglietti, 2014; Giordano, 2009; McCallum et al., 2020; OECD, 2011; Sharma, 2009; WWAP, 2015).

However, groundwater depletion is a significant issue globally, and it is estimated that over 20% of the world's aquifers are overexploited (Gleeson et al., 2012; Richey et al., 2015; Wada et al., 2010). Use of groundwater and its eventual depletion is not an isolated problem, and entails various side effects, including land subsidence (Erban et al., 2014; Farr & Liu, 2015; Galloway & Burbey, 2011), coastal saltwater intrusion (Ferguson & Gleeson, 2012; Konikow, 2011; Michael et al., 2017; Werner & Simmons, 2009), decreased baseflow and consequent basin salinization (Farber et al., 2004; Pauloo et al., 2020; Warner et al., 2013), desertification (Sheridan, 1981; Van Dijck et al., 2006; Yang et al., 2015), and increased political conflict across transboundary aquifers (Giordano, 2009; Jarvis et al., 2005; Wolf, 2007; Zeitoun & Mirumachi, 2008). The Intelligence Community Assessment (NIC, 2012) has identified water stress to be a potential driver of regional instability. Therefore, understanding the availability of groundwater in the world's aquifers as it is exploited by humans over time is a key component for decision-makers interested in populations at risk of drought and consequent conflict.

Yet, as of 2022, despite its critical role in the global water cycle, in trade, and in climate, groundwater is underrepresented in current United Nations' Sustainable Development Goals (Gleeson et al., 2019; Guppy et al., 2018). This negligence often arises from its "invisible" (Edmunds, 2004) or hidden (Chapelle, 1997; Eckstein, 2005) nature. Groundwater storage and fluxes are also generally poorly monitored due to the challenges in obtaining information on a fluid that is at depth below the ground surface. Our understanding of ground water usage and availability often derives from limited or sparse in situ measurements, which can be problematic to obtain globally and especially in denied access areas. In situ measurement techniques, such as groundwater well monitoring, are further complicated by diverse and heterogeneous geology and the resulting spatial heterogeneity in soil type, texture, aquifer structure, and specific yield (Berg & Illman, 2011; Gleeson et al., 2011; Meinzer, 1932; Upton et al., 2019; van Bussel et al., 2015). Even in locations where in situ data are plentiful (e.g., California's Central Valley, Faunt, 2009), there are challenges in the aggregation, integration, and interpretation of these observations. For data-poor or contested regions, information on groundwater depletion can be nonexistent.

For these reasons, remote sensing approaches to monitoring groundwater or aquifer change can be advantageous (Becker, 2006). Satellite and airborne observations have revolutionized the understanding of hydrology and water availability at regional to global scales in ways that would not have occurred with relatively sparse in situ observations. Earth-observing satellites and airborne systems can provide both the "big picture" spatial coverage as well high-resolution proxies for groundwater storage change and aquifer structure over large regions. This Earth sensing data revolution has the potential to provide the regional to global understanding essential for improving predictive models and informing policy makers, resource managers, and the general public (Famiglietti et al., 2015). In recent years, several space- and air-borne remote sensing methods have been applied to the study of groundwater, demonstrating that water storage, extraction, and recharge, as well as aquifer hydrostratigraphy, can be estimated under the right circumstances on regional to global scales. Yet, challenges remain in using these data sets, particularly in relating the raw observed data to hydrologic variables of interest, in downscaling coarse data sets, and in integrating diverse remotely sensed data sets into groundwater models. In this work, we review the principal groundwater (and groundwater/aquifer proxy) measurement techniques that have been developed, including gravitational techniques, InSAR, lidar, airborne electromagnetic (AEM) systems, and GNSS. We also discuss future needs and research directions both in measuring and modeling capabilities, noting that integrating multiple remotely sensed data sets into groundwater modeling frameworks is an area of significant opportunity.

2. Technological Progress and Current Limitations

This section explores the technologies and techniques that are applicable to the groundwater proxy measurements. They include gravity measurements (e.g., Gravity Recovery and Climate Experiment (GRACE) and GRACE-FO; Tapley et al., 2004; Rodell et al., 2007; Famiglietti et al., 2011), InSAR measurements of surface displacements (Amelung et al., 1999; Farr & Liu, 2015; Galloway et al., 1998; Reeves et al., 2014), Global Navigational Satellite System (GNSS) measurements of surface displacements at points (Amos et al., 2014; Argus et al., 2014, 2017; Borsa et al., 2014; Enzminger et al., 2019), radar altimetry (Hwang et al., 2016), lidar (An, 2015), subsurface aquifer sounding (Heggy & Paillou, 2006; Mukherjee et al., 2010), and infrared/thermal measurements of evapotranspiration as a proxy for ground water use in areas known to rely on groundwater as a water source (Chen & Hu, 2004; Jackson, 2002; Maxwell et al., 2007) (Table 1). In this review, we describe the measurement principle and algorithmic approach to transforming the measurement into a measure of groundwater, the trade space for systems that can achieve measurements, and their strengths and limitations.

2.1. Gravity-Based Measurements of Groundwater

The GRACE mission has provided estimates of the time-variable gravity field spanning April 2002–June 2017 (Figure 1; Tapley et al., 2004; Rodell et al., 2018; Famiglietti et al., 2011; Richey et al., 2015). These measurements are now being continued with the successful launch of the GRACE Follow-On (GRACE-FO) mission in May 2018, which was designed primarily as a continuity mission (Landerer et al., 2020).

Unlike most remote sensing measurement approaches, the GRACE and GRACE-FO missions are nontraditional in that there is no instrument pointed at the Earth taking measurements. Rather, the basic mission architecture consists of a pair of identical satellites flying in a leader-follower formation, separated by approximately 220 km in the along-track direction (Figure 2). The primary instrument is a K/Ka band microwave ranging instrument

Table 1
Summary of Techniques Presented in Section 2

Technique	Capabilities	Advantages	Disadvantages
Gravimetric measurements	GRACE and GRACE-FO: Measures groundwater storage change using gravimetric measurements at a $(300\ km)^2$, 30-day resolution.	Can obtain a global picture of groundwater storage anomalies.	Spatial scale makes it difficult for usage in smaller aquifers without additional modeling, and high frequency mass variations are not captured.
Surface deformation measurements	Tracks ground movement to estimate changes in groundwater storage. Deformation is driven by changes in pore pressure and effective stress as groundwater storage changes. InSAR: mm-scale changes can be recorded in meter-scale track resolutions. GNSS: Provides point-based measurements but stations exist globally. Radar altimetry: >1 cm/yr vertical scales along 1-km track resolutions. Lidar: 3 cm vertical scales in 1-km grids (ICESat-2).	Can provide continuous records of surface deformation. High temporal and spatial resolution (or station density, in the case of GNSS) allows for robust applications at various scales.	A good constraint of geologic characteristics is needed to accurately relate nonlinear surface deformation responses to groundwater storage changes.
Airborne Electromagnetic Systems (AEM)	Electrical conductivity is measured to estimate water table. Shallow (1–3m) and deep (300–400m) aquifers can be surveyed.	Can rapidly survey large areas at a low cost.	Geologic properties of the aquifer system need to be well-constrained. Limited capacity in saline systems.
Proxy measurements	Soil moisture and evapotranspiration can be used as proxies to groundwater use in regions that have vegetation reliant on groundwater (e.g., arid regions, pumping/irrigation regions, and high-infiltration regions).	Optical remote sensing methods are often high in spatial resolution, allowing this technique to be applied at local scales.	Relies on an inferred relationship between vegetation and groundwater use (conjunctive use of surface water not considered).

(MWI) that measures how the distance changes between the satellites to micron-level precision as they orbit the Earth. As the satellite pair approaches a gravity (or mass) anomaly, the leading satellite "feels" this local gravitational attraction, and accelerates relative to the trailing satellite, resulting in a change in distance between the satellites. After the first satellite flies over this anomaly, it is then decelerated back toward the anomaly while the trailing satellite is accelerated toward it, again resulting in a relative range change. The pair of satellites continues this elegant tango as they orbit the Earth in tandem, continuously tracking the relative range between them. It is worth mentioning that while the GRACE-FO mission was primarily designed as a continuity mission for GRACE, it does carry a prototype laser interferometer to measure the range changes between the satellites approximately 100 times more precisely than GRACE (approximately 10 nm). This technology can be viewed as an enabling technology for future missions, as other error sources currently limit the spatial and temporal resolution of the derived gravity fields.

GRACE and GRACE-FO canonically provide monthly estimates of the time variable geopotential field of the Earth. These measurements of geopotential are then converted to a corresponding height of a thin layer of water on the Earth's surface (units: equivalent water height (EWH)), using the methods of Wahr et al., 1998 or Rowlands et al., 2005. The accuracy of GRACE is approximately 2 cm EWH over a region $(300\ km)^2$ at monthly timescales. Removing an arbitrary time mean from the series of GRACE measurements allows for calculation of total water storage anomalies (TWSA) from the data. It is important to note that the GRACE-based measurements of TWSA can be contaminated by solid Earth mass variations. Users interested in isolating subsurface mass variations (such as changes in groundwater), must remove changes in the solid earth mass variations (e.g., from earthquakes and glacial isostatic adjustment processes) using models (Han et al., 2008; Peltier et al., 2018). After removal of solid

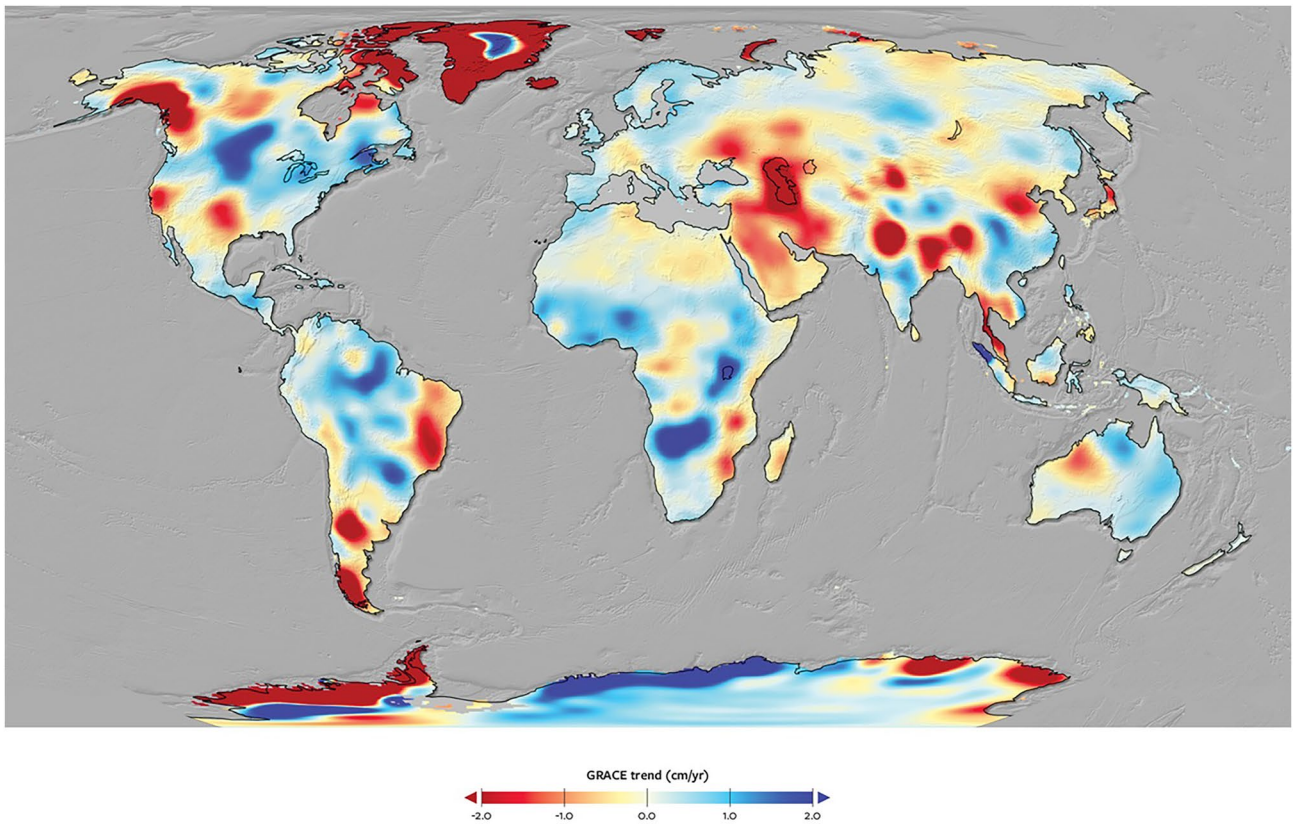

Figure 1. (From Famiglietti, 2019, based on Rodell et al., 2018). Global trends in terrestrial water storage (cm/yr) as observed from Gravity Recovery and Climate Experiment (GRACE) between April 2002 and March 2016.

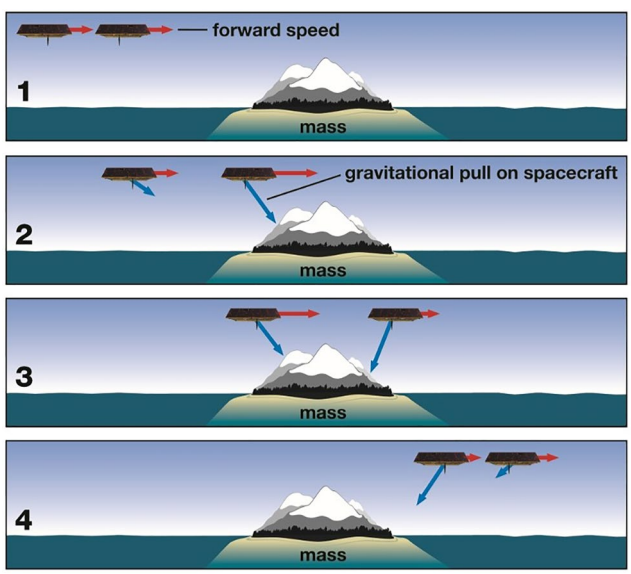

Figure 2. (From NASA) How Gravity Recovery and Climate Experiment (GRACE) and GRACE-FO measures gravity. The two satellites travel together maintaining a relatively constant distance of 220 km between each other. As the satellites fly over a region of gravitational attraction, the acceleration of the satellites is measured and converted back to equivalent gravitational mass.

Earth effects, TWSA then contains information on the integrated water storage change for a region, including changes in surface water (lakes and rivers; $\Delta W_{surface}$), vegetation and canopy water (ΔW_{veg}), soil moisture (ΔW_{soil}), snow (ΔW_{snow}), evapotranspiration (ΔW_{ET}), and groundwater (ΔW_{ground}). In order to isolate a groundwater signal, the TWSA needs to have estimates of each of the other variables removed (Equation 1):

$$\text{TWSA} = \Delta W_{surface} + \Delta W_{veg} + \Delta W_{snow} + \Delta W_{soil} + \Delta W_{ground} \quad (1)$$

Typically, these estimates are provided by a hydrology model, in which precipitation and radiative forcing, as well as soil composition are used to calculate the water balance, including storage change, evapotranspiration and runoff, over a discretized control volume (i.e., a model grid cell). This is typically done with land surface model outputs that readily produce estimates of snow water equivalent and soil moisture (Rodell et al., 2007), but it can also be accomplished using observations where they are available (Yeh et al., 2006). Surface water storage changes are significant in the wet tropics and in certain high latitude regions (Getirana et al., 2017), and estimates may come from in situ stage observations or satellite altimetry, as available. Canopy and vegetation water change is typically assumed small and as such often neglected (Rodell et al., 2005). However, it is important to note that land surface model errors will accumulate in the groundwater residual calculated from TWSA, and careful error accounting must be performed (Rodell et al., 2007). The uncertainty in month-to-month TWSA-model groundwater

residuals is typically substantial, but the approach can be useful in identifying long-term trends in groundwater depletion (Rodell et al., 2009).

Limitations of GRACE and GRACE-FO lie in data processing errors, orbital altitude limitations, and observation geometry. Data processing is a critical component in resolving time-variable gravity. After a month of accumulating onboard measurements, a realistic simulation of satellite orbits propagating through a dynamic Earth system is set up, creating synthetic intersatellite range measurements. The created dynamic earth system must include force models of high frequency mass variations, such as ocean tides, high frequency atmosphere, and dynamic ocean mass variations. Since measurements must be accumulated for ∼30 days for a stable solution, GRACE cannot resolve these high frequency mass variations, and as such, a model must be used to account for their effect on the orbits of the two satellites. Model errors then alias into the monthly gravity solution as "temporal aliasing errors," and have a greater effect on gravity retrieval than the expected measurement system errors (combination of MWI, accelerometers, star cameras, and Global Positioning System (GPS)) onboard the GRACE-FO satellites (Wiese, Visser, & Nerem, 2011). Satellite altitude is also a noteworthy limitation of GRACE and GRACE-FO. The GRACE and GRACE-FO satellites were placed in an orbit with an altitude of approximately 500 km, which naturally decays due to atmospheric drag. As the satellite orbits decay, the sensitivity to the gravity field perturbations increases. While lower altitudes would allow for a spatial resolution finer than 300 km, this would increase atmospheric drag, thereby limiting the lifetime of the mission. The final limitation worth noting is the observation geometry. GRACE and GRACE-FO are placed in a polar orbit (for global coverage), and take measurements solely in the along-track direction. Because of this, there is limited information on any east-west gravity variations, and both measurement system errors and temporal aliasing errors are manifest as longitudinal stripes in the gravity solution. The user community has become adept at removing them via a wide variety of post-processing filters (Luthcke et al., 2013; Save et al., 2016; Swenson & Wahr, 2002; Watkins et al., 2015). However, in any approach of removing the stripes, users run the risk of removing real geophysical signal as well. In fact, a set of so-called "scaling factors" are recommended to implement for most users to restore lost geophysical signal due to the filtering (Landerer & Swenson, 2012; Wiese et al., 2016).

The GRACE record provides a roughly 15-year observational period globally, while the GRACE-FO mission is extending that record into the 2020s. Continuity with future satellite gravimetry missions will be vital to extend this valuable record and determine with more certainty the long-term rates of groundwater depletion, potential climate change impacts, and responses in human activity to periodic events such as droughts.

2.2. Surface Deformation Measurements

Time series analysis of surface subsidence and uplift in regions of exploited aquifers with compressible sediments has been used to estimate changes in groundwater storage (both due to recharge and withdrawal). Radar altimetry, Lidar, Interferometric Synthetic Aperture Radar (InSAR; ground displacement measured using interferometric pair maps; see Section 2.2.1), and GNSS are able to measure surface deformation at high vertical precision (Sneed, 2001). In areas of susceptible geology, groundwater pumping can cause compaction of certain layers, yielding elastic or inelastic subsidence at the surface (Amelung et al., 1999; Argus et al., 2005; Bawden et al., 2001; Chaussard et al., 2013, 2014; Smith et al., 2017).

The deformation is driven by a change in pore pressure in subsurface sediments, which causes a change in effective stress of the opposite sign (Terzaghi, 1925). An increase or decrease in effective stress causes the aquifer matrix to either consolidate or expand, respectively. It is often more convenient to refer to effective stress changes as changes in groundwater levels, which are related to pore pressure through a unit conversion (Fetter, 2001). Increasing groundwater levels cause a decrease in effective stress and expansion of aquifer material, while decreasing groundwater levels causes the opposite to occur.

The amount the matrix deforms per unit change in groundwater level is a function of the compressibility and stress history of the layer that is deforming. Fine-grained, unconsolidated materials such as clays are highly compressible, and typically deform much more than coarse-grained or consolidated materials. When the groundwater level drops below the lowest level previously experienced by the deforming material, or pre-consolidation head, inelastic, or non-recoverable consolidation occurs (Riley, 1969). At all other times, the deformation is elastic. Typically, inelastic deformation per unit change in groundwater level is one to two orders of magnitude greater than elastic deformation (Helm, 1975; Riley, 1969). Thus, the key common factors that typically result

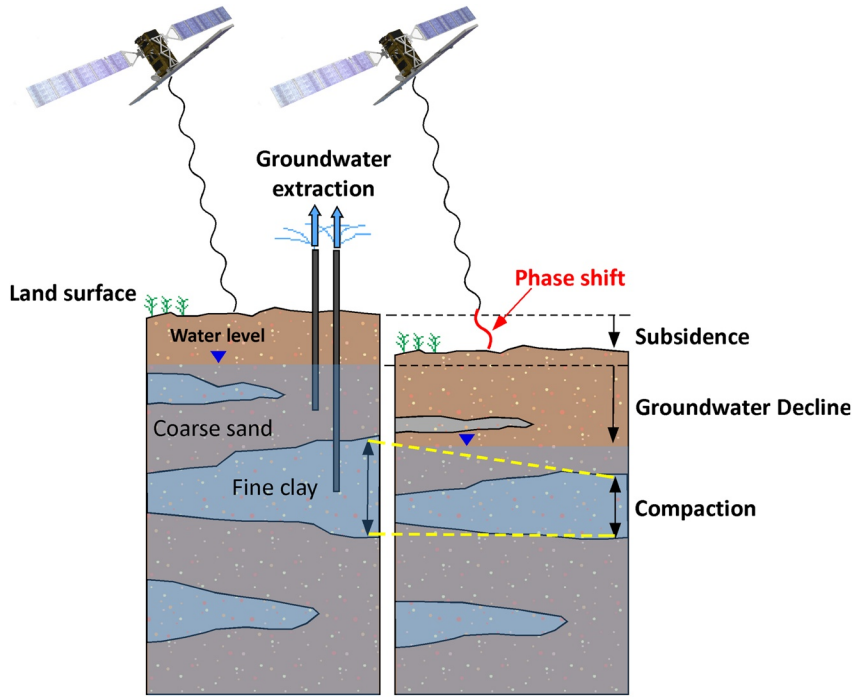

Figure 3. InSAR measures surface deformation by measuring the difference in the phase of the radar wave between the two passes if a point on the ground moves and the spacecraft is in the same position for both passes. Because changes to groundwater subsequently causes elastic or inelastic surface response, InSAR can be used to infer volumetric groundwater change by measuring surface deformation.

in a large amount of subsidence due to groundwater pumping are: (a) a historically large drop in groundwater levels and (b) thick, unconsolidated, and compressible sediments, such as clays. Because multiple factors can cause deformation and because there is significant spatial variation in both how groundwater levels respond to changes in groundwater storage and how much deformation occurs for a given change in groundwater level, linking geodetic observations with changes in groundwater storage is challenging. To do this successfully, one must account for the nonlinear processes described above, as well as the spatial variation in aquifer thickness and compressibility. In spite of these challenges, many rich geodetic data sets are currently available that have been used to estimate aquifer properties in a number of studies.

Global Navigational Satellite System can provide measurements that are continuous in time at the station locations (Bürgmann et al., 2006; Dehghan-Soraki et al., 2015; Ferretti et al., 2007). Interferometric Synthetic Aperture Radar and radar altimetry can provide a continuous map of the deformation, observed whenever the satellite or aircraft covers the area. Land deformation can therefore serve as a proxy for volumetric groundwater change. However, as surface response to groundwater change can be nonlinear and spatially heterogeneous, such approaches are best used when complemented by knowledge of the geologic and general hydrologic properties of the aquifer.

2.2.1. Interferometric Synthetic Aperture Radar

Interferometric synthetic aperture radar (InSAR) for measuring surface deformation was first demonstrated using the L-band SEASAT satellite by Goldstein et al. (1988). Since then the technique has become a major geodetic tool for measuring surface deformation and change in a variety of disciplines, including geophysics (Hooper et al., 2004; Wright et al., 2004), climate science (Gourmelen et al., 2011; Zhao et al., 2016), hazard assessment (Chen et al., 2012), and infrastructure monitoring (Eppler & Rabus, 2012; Milillo et al., 2016; Sneed, 2001). Particularly for areas where local in situ measurements are difficult or impractical, spaceborne InSAR has proven to be essential.

Interferometric SAR takes advantage of the coherent nature of SAR imaging. Each image comprises complex-valued pixels, each representing a coherent backscatter amplitude and phase. As illustrated in Figure 3,

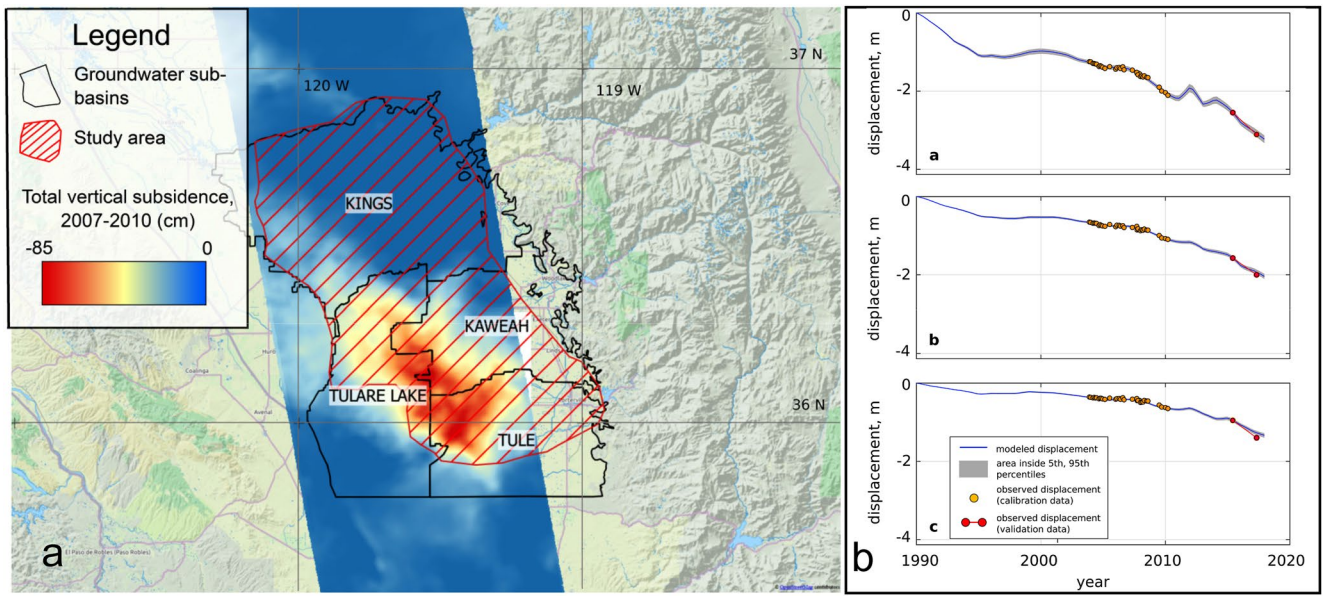

Figure 4. (Modified from Smith et al., 2017 and Smith & Knight, 2019). (a) Map of InSAR-derived total vertical subsidence from June 2007 to December 2010 across several groundwater sub-basins in Central Valley, California. (b) Modeled and observed deformation data, with modeled subsidence (blue line), error (gray), InSAR-derived deformation from Envisat and ALOS (orange; used for calibration), and total displacement from Sentinel-1 (red; excluded from calibration, but used for validation) for three locations within the Kaweah sub-basin.

an InSAR satellite passing over a location before and after a surface motion such as subsidence due to subsurface fluid withdrawal, at exactly the same point in inertial space, measures how the ground shifts between passes, via a radar interferogram. This is the product of the first image with the complex conjugate of the second (Donnellan et al., 2008). The interferogram measures the difference in phase of the radar wave between two passes, which is sensitive to ground motion directed along the radar line of sight. An InSAR image of the point-by-point phase difference of the wave on the surface is used to create a map of the movement of the surface over time. In this way, ground deformation along the line-of-sight (LOS) direction on the scale of a fraction of the radar wavelength can be resolved as long as the phase coherence between the signals is maintained (Gabriel et al., 1989; Zebker & Goldstein, 1986). The radar instrument can take observations through cloud cover, without sunlight, and can measure sub-centimeter changes. Effective use of InSAR often relies on a time series of observations, and with the current ubiquity of civil and commercial SAR systems acquiring global data, the reliability, accuracy, and usability of these products have greatly improved. For groundwater estimation, where changes occur slowly, time series measurements can be essential, particularly for systems with short wavelengths like X-band (3 cm wavelength) where changes in other surface properties such as vegetation or soil moisture reduce coherence and introduce noise, so stacking many observations over time is needed to track the signal.

Successful application of InSAR for groundwater estimation is contingent on local geology, surface cover, and atmospheric and ionospheric noise. For subsidence to be employed as a proxy for changes in groundwater storage, the aquifer must undergo physical deformation associated with groundwater depletion or recharge. Therefore, the spatial pattern and extent of surface subsidence is contingent upon geologic heterogeneity, matrix elasticity, effective stress, and the critical head threshold (Castellazzi et al., 2016; Hoffmann et al., 2003). Nonetheless, subsidence-inferred groundwater changes have been published for many areas globally, including Iran (Jafari et al., 2016; Motagh et al., 2017), India (Chatterjee et al., 2006), Mexico (Calderhead et al., 2009), China (Zhou et al., 2016), and the United States (Argus et al., 2005; Bawden et al., 2001; Chen et al., 2017; Farr & Liu, 2015; Liu et al., 2019; Reeves et al., 2011; Smith & Majumdar, 2020) (Figure 4).

Because InSAR relies on the coherent nature of the backscattered energy, if surface features change their relative position within a pixel (as opposed to a bulk shift within the pixel), an interferometric measurement cannot be made. Therefore, vegetation cover or changes in the surface due to agricultural activity can also lead to decorrelation of the InSAR signal (Castellazzi et al., 2016). However, these issues can be addressed by using longer wavelength radars that are less sensitive to such changes or by observing more often. Precipitable water vapor

Table 2
List of Current Synthetic Aperture Radar (SAR) Operations That Could Be Utilized for Groundwater Applications

System	Operational Period	Wavelength/Polarization	Temporal Sampling	Global Coverage Strategy
Sentinel-1 (ESA/EU)	2015-present	C-band (5.6 cm) Single/Dual	6 or 12 days, area dependent	Mostly global at 12-day repeat. Europe and selected areas at 6-day repeat. Usually Ascending or Descending orbit acquisition, not both.
ALOS-2	2016-present	L-band (24 cm) Single	14 days capable, generally 5–6 samples per year	Global maps roughly yearly, Ascending or Descending.
Radarsat-2	2007-present	C-band (6 cm) Single/Dual/Quad	12 days, area dependent	Fully commercial system.
COSMO Skymed	2013-present	X-band (3 cm) Single/Dual/Quad	4, 8, 12, or 16 days, area dependent	Some wide-area campaigns (e.g., Italy and California) but generally targeted observations for specific commercial, scientific, or military purposes.
TerraSAR-X/Tandem-X	2010-present	X-band (3 cm)	11-day repeat	Global mapping for topography has used much of its duty cycle. Targeted studies always possible.

in the atmosphere can also be a limiting factor particularly in humid areas, as centimeters of path delay can lead to an error in the deformation signal. Typically, many samples over time are needed to average out this noise source, since the water vapor delays are uncorrelated from time to time, while the aquifer deformation is highly correlated to secular or seasonal trends (Li et al., 2009, 2012). For longer wavelength systems such as the C- or L-band (5 and 25 cm wavelength, respectively), the ionosphere can additionally introduce significant path errors and require corrective methods using the data themselves (Meyer, 2011). The optimal InSAR data product to be used for groundwater evaluation therefore depends on the regional geologic, vegetation, and climatological characteristics. Current operational SAR systems are listed in Table 2.

Limitations to using InSAR in application and resolution of groundwater problems lie in data availability, repeat coverage, and sampling. For global groundwater monitoring, only Sentinel-1 from the European Space Agency (ESA) provides sufficient coverage and repeat coverage suitable for a global assessment. Nonetheless, changes to aquifers occur at low spatial gradients over longer timescales. Hence, InSAR products with modest spatial resolution (100's of meters) images sampled on weekly timescales over time can readily be utilized to observe surface deformations related to groundwater storage changes.

2.2.2. Global Navigational Satellite System (GNSS)

In groundwater applications of GNSS, observations are collected "in situ" from receiving stations on the Earth surface, in proximity to the region of interest. By the strictest definition, active tracking of GNSS on the ground is not a remote sensing technique. At the same time, GNSS is a well-established spaceborne measurement technique that leverages a robust and expanding space segment of navigation satellites for highly accurate positioning. Most importantly, terrestrial GNSS applications rely on a vast network of low-cost, geodetic-grade ground receivers deployed for a variety of scientific applications. These "sites of opportunity" imply that dedicated in situ resources are not necessary for the most groundwater applications. For these reasons and the complementary nature of these measurements with more traditional remote sensing observations, in this paper, we consider the important role of GNSS in monitoring groundwater variations.

We note that GNSS refers to a broad range of satellite-based positioning systems, one of which is the GPS of the US. The past decade has witnessed a dramatic proliferation of science-grade GNSS stations around the globe, each of which can be considered a station of opportunity for monitoring groundwater. Blewitt et al. (2018) describes this as an "exponential explosion" of geodetic-quality stations, and now routinely process open-access GNSS data from over 17,000 globally distributed sites. The notion of GNSS stations as a sparse grid is rapidly giving way to a new paradigm of interconnected dense GNSS arrays spanning the globe (Figure 5). While the most noteworthy dense arrays are in the United States, Japan, Europe, and other areas of strategic interest (e.g., South America, sub-Saharan Africa, and Turkey) are increasingly represented by denser GNSS networks. Time series of GNSS station positions are available through the Nevada Geodetic Library (http://geodesy.unr.edu/PlugNPlayPortal.php), and are built from daily point positions with typical repeatabilities of 2, 2, and 4 mm in latitude, longitude, and height, respectively. This level of precision enables accurate monitoring of surface

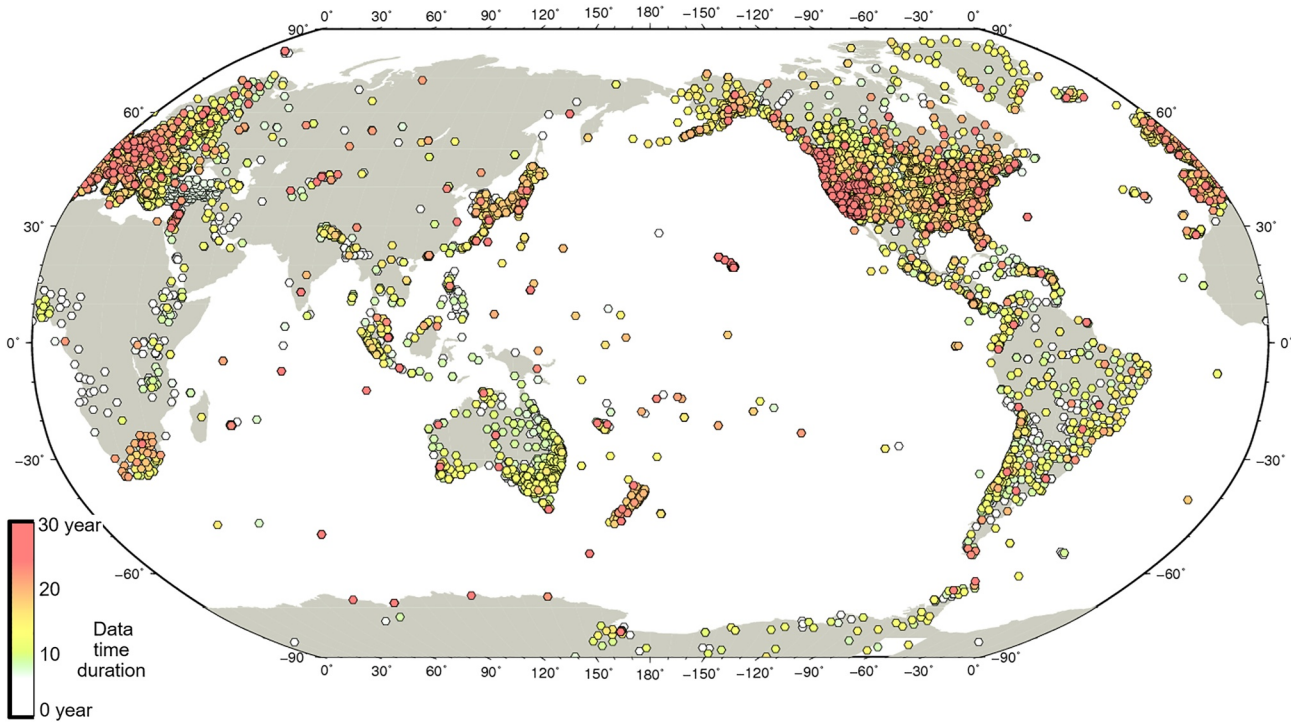

Figure 5. GNSS sites (hexagons) between 3 and 28 years of data analyzed by the Nevada Geodetic Laboratory (Blewitt et al., 2018) with which to evaluate change in total water storage using displacements of Earth's surface. The color filling each hexagon denotes the time duration of data at a site (see legend).

deformation, which reflects changes in groundwater among other phenomena (e.g., Argus et al., 2014). The GNSS time series can also be assimilated into models and/or combined with other observational data sets (e.g., with GRACE and InSAR; see Section and Liu et al., 2019) to complement point-based measurements of surface deformation.

Global Navigational Satellite System stations provide continuous, accurate point measurements of vertical movements of the Earth surface, including those linked to depletion and replenishment of groundwater and other fluids in the crust. With dense networks of GNSS stations, vertical deformations can be characterized at high spatial resolutions to monitor regional variations in groundwater and probe potential causes. The southwestern U.S. is an example of a region that hosts a dense network of GNSS stations, providing indirect measurements of groundwater supply at depth. The Central Valley of California, which produces more than half of the nation's produce and generates more than $17 billion in agricultural profit per annum (Hastings, 2014), has suffered significant subsidence resulting from groundwater overdraft. Global Navigational Satellite System stations in the Central Valley are located mainly on compressible unconsolidated aquifers and record subsidence related to aquifer compaction from groundwater depletion (Figure 6). Interestingly, elastic response was recorded in the stations surrounding the valley, in the California coastal ranges and in Sierra Nevada (Figure 6). This was potentially attributed to unburdening of the lithosphere from groundwater pumping (Amos et al., 2014) or drought-driven losses of groundwater and deep soil moisture, especially in recent years (Argus et al., 2017). Both explanations underscore the remarkable ability of dense GNSS networks to provide insight on groundwater variations. It also highlights the advantage of GNSS networks, as GNSS stations do not need to lie directly over the particular aquifer of interest to detect changes. While GNSS stations located within the Central Valley are recording subsidence in response to aquifer compaction, nearby stations record elastic rebound in response to unloading. As such, fingerprints of groundwater depletion extend well beyond the margins of the aquifer system, and the water loss can be inferred from the size of the elastic load signal assuming that other sources of vertical deformation, such as tectonics and volcanic activity, can be modeled or removed. Recently, White et al. (2022) also reviewed in detail GNSS applications in hydrogeodesy, including how hydrologic storage changes can be isolated from GNSS observations of surface displacement.

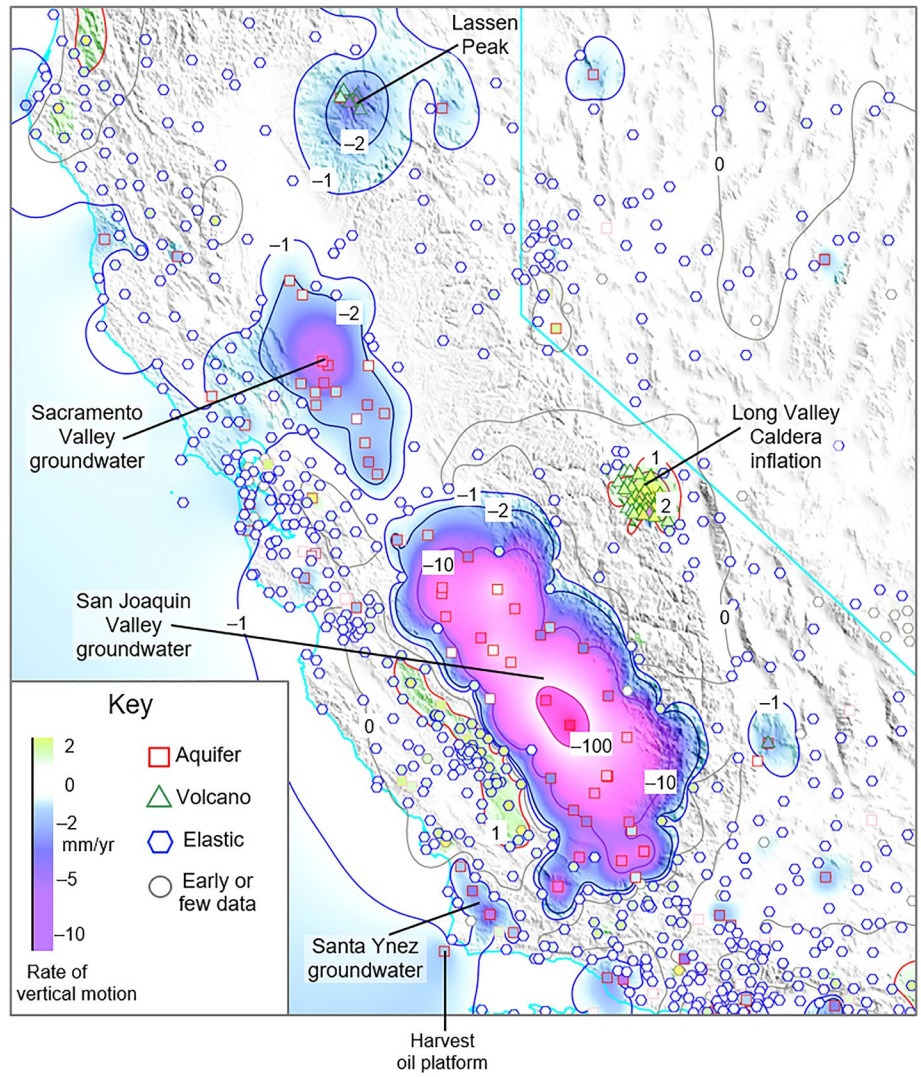

Figure 6. Mean rate of vertical motion estimated from Global Navigational Satellite System (GNSS) data from 2006 to 2021. Color gradations represent the rate of vertical motion: very fast subsidence (magenta), slow subsidence (blue), nearly zero vertical motion (white), and slow uplift (green yellow). Contours area at 2, 1, 0, −1, −10, and −100 mm/yr. Blue hexagons are GNSS sites recording primarily solid Earth's elastic response to change in water at Earth's surface. Red squares are GNSS sites recording the Earth's porous response to change in groundwater. Green triangles are GNSS sites influenced by volcanic activity. GNSS sites are assigned to the different categories following Argus et al. (2017). Vertical rates of motion are estimated from GNSS positions as a function of time determined by the National Geodetic Laboratory (Blewitt et al., 2018; Hammond et al., 2021) using satellite orbits and clocks determined by Jet Propulsion Laboratory (Bertiger et al., 2020). Santa Ynez groundwater indicated in the figure spans the Santa Ynez basin (southern half) and the Santa Maria River Valley groundwater basin (northern half).

Examples of groundwater detection from GNSS can be also readily found near regions of highly variable gravity. Figure 7 (top) shows the locations of selected GNSS ground stations against the backdrop of time variable gravity, as expressed as RMS variability of the GRACE (RL05) monthly product. Comparison of the GRACE signal to the GNSS record shows remarkable agreement between the two measurements. As such, GNSS measurements are useful in providing long-term subsidence records for various regions around the world, and in correlating groundwater storage changes from GRACE to surface deformation and response.

2.2.3. Radar Altimetry for Surface Deformation

While altimetry missions were originally designed for oceanic and cryospheric applications, radar altimetry can also detect groundwater-related subsidence, providing an indirect measurement of groundwater storage changes

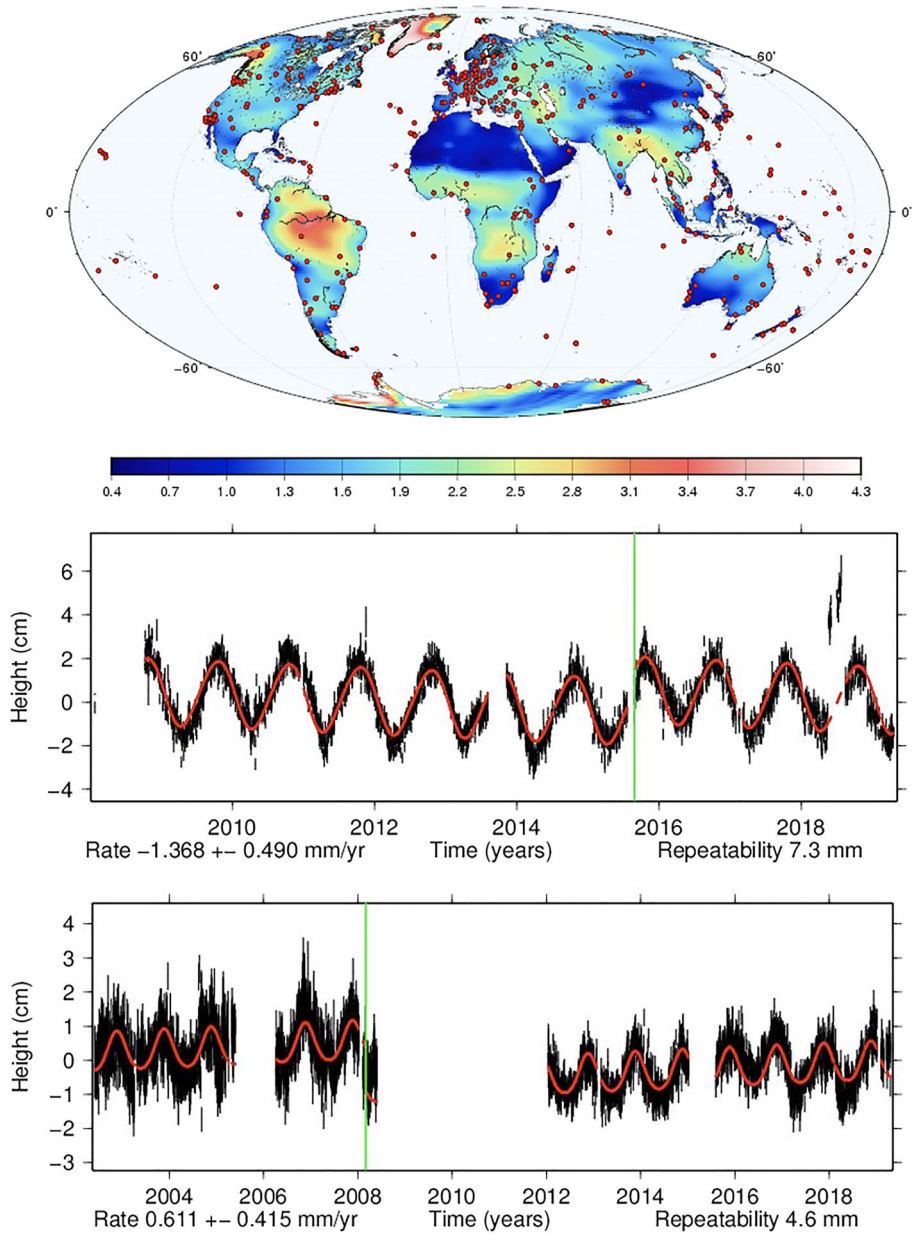

Figure 7. Top, Locations of selected Global Navigational Satellite System (GNSS) stations (red dots) from the International GNSS Service plotted against the RMS variability of gravity from Gravity Recovery and Climate Experiment (GRACE) (colors); Middle (http://sideshow.jpl.nasa.gov/post/series.html), GNSS station in Porto Velho, Brazil (black) and GRACE (red); and Bottom, GNSS station in Lusaka, Zambia in the Okavango river basin (black) with GRACE (red).

(Hwang et al., 2016). In contrast to InSAR that uses interferometry between emitted and reflected waveforms, radar altimetry uses nadir echo of radar pulses to measure two-way travel time delay to estimate surface elevation changes (Hwang et al., 2016; Kuo et al., 2015). Flat croplands produce altimeter waveforms with a steep leading edge, similar that of a calm lake surface, which can be retracked to quantify subsidence. Because it does not require highly temporally correlated ground features like InSAR, altimetry is not as spatially limited and can provide long-term records of subsidence.

In 2016, Hwang et al. showed successful quantification of long-term subsidence in cropland areas of California, China, and Taiwan, using TOPEX/POSEIDON, JASON-1, ENVISAT, and JASON-2. The three regions have been extensively studied using extensometers, GNSS, and InSAR, but often such data sets are spatially or

temporally limited. Altimetry was therefore able to complement the existing data sets with wide spatial coverage and long-term monitoring records. Subsidence rates from altimetry agreed well with rates from other measurement methods, such as precision leveling and GNSS. Current altimetry technologies are capable of resolving subsidence at a 1-km along-track spatial resolution, at >1 cm/yr vertical scales. In regions where groundwater availability is known to be the main driver of subsidence, altimetry could serve as a useful tool for groundwater approximation, especially by utilizing missions with a long repeat period and small cross-track spacing. However, it is important to note that this approach would be best applied when measuring subsidence on flat terrains, where vegetation is shorter and has minimal buildings within the footprint.

2.2.4. Lidar

Lidar is another method of detecting land elevation change as a proxy for groundwater extraction. NASA's ICESat (2003–2006) and ICESat-2 (2018-present) are earth-observing spacecraft with laser altimeters to measure ice sheet elevation, sea ice thickness, as well as vegetation height, bathymetry, and terrestrial topography (Abdalati et al., 2010). NASA's ICESat (2003–2006) demonstrated land surface heights with accuracy as good as 2 cm, with 3 cm vertical precision, over the ideal surfaces of Bolivian salt flats (Fricker et al., 2005). With a 60-m nadir footprint from a 600 km altitude, ICESat imaged points on a line, not in a push-broom fashion, making its grid dense along-track but coarse across-track. The successor ICESat-2, launched in 2018, delivers gridded 1-km maps of land and vegetation height for select target areas. While similar in power and mass to the original ICESat at 300 W and 300 kg, it has a much higher along-track resolution of 0.7 m. Since both ICESats sample points along their ground track, rather than sweeping their beams over a field of view, the surface map is synthesized from multiple overflights of the same area, with slightly varying ground tracks. Satellite lidar measurements are made from around 100 photons per spot, where a spot is on the order of 40 m in diameter. The lowest-level ICESat-2 products that include land height are resampled at 100 m intervals along the satellite ground track.

In 2015, a successful application of ICESat in the North China Plain was observed to quantify land subsidence associated with groundwater depletion measured from GRACE (An, 2015). Contribution of vegetation height to the ICESat signal was also assessed using Normalized Difference Vegetation Index from NASA's Moderate Resolution Imaging Spectroradiometer. As such, it is customary for land surface measurements to be used in conjunction with GRACE data sets to get a holistic picture of groundwater usage and its related aquifer response.

2.3. Airborne Electromagnetic Systems

AEM systems are fast, low-cost methods of surveying large-scale, shallow (1–3 m) to deep (300–400 m) aquifer systems using the measured response from an active electromagnetic source to estimate the subsurface electrical conductivity (Paine & Minty, 2005; Siemon et al., 2009). First introduced in the 1950s for mineral exploration (Baudouin et al., 1967; Collett, 1967), AEM was successfully applied to groundwater investigation in Spikeroog, Germany in 1981 (Sengpiel & Meiser, 1981), and has increasingly been used for groundwater systems. Due to its dependence on electrical conductivity, AEM is sensitive to water table elevations, geologic properties of the aquifer (particularly the interfaces between resistive materials such as bedrock, moderately resistive materials such as sands, and conductive materials such as clays), and salinity distributions (Abraham & Cannia, 2011; Dewar & Knight, 2020; Kirsch, 2006; Knight et al., 2018; O'Connell et al., 2020). In particular, saline water delineations using AEM have been used in various field settings, including coastal regions with saltwater intrusion (Fitterman & Deszcz-Pan, 1998; Goebel et al., 2019; Gottschalk et al., 2020), aquifers with salt contamination (Ball et al., 2020; Cresswell et al., 2004; Siemon et al., 2019; Smith et al., 1992), and regions with produced water from oil and gas extraction (Paine, 2003). However, for saline, high conductivity systems, measurements are typically limited to tens of meters (Spies & Woodgate, 2003).

AEM systems operate by generating electric currents through coils (Figure 8). As these currents change, either by being shut off rapidly or alternated, ground-penetrating magnetic fields are produced, producing eddy currents in the subsurface. A secondary electromagnetic field, the strength of which is a function of the distribution of subsurface conductivity, is generated from these eddy currents, and is then detected by the receiver coils (Palacky, 1993).

There are two different methods for acquiring AEM data: the frequency-domain method and the time-domain method. Systems with the frequency-domain method generate an alternating current at a limited number of frequencies (typically ranging from one to six Hz, i.e., Minsley et al., 2021). This current runs continuously

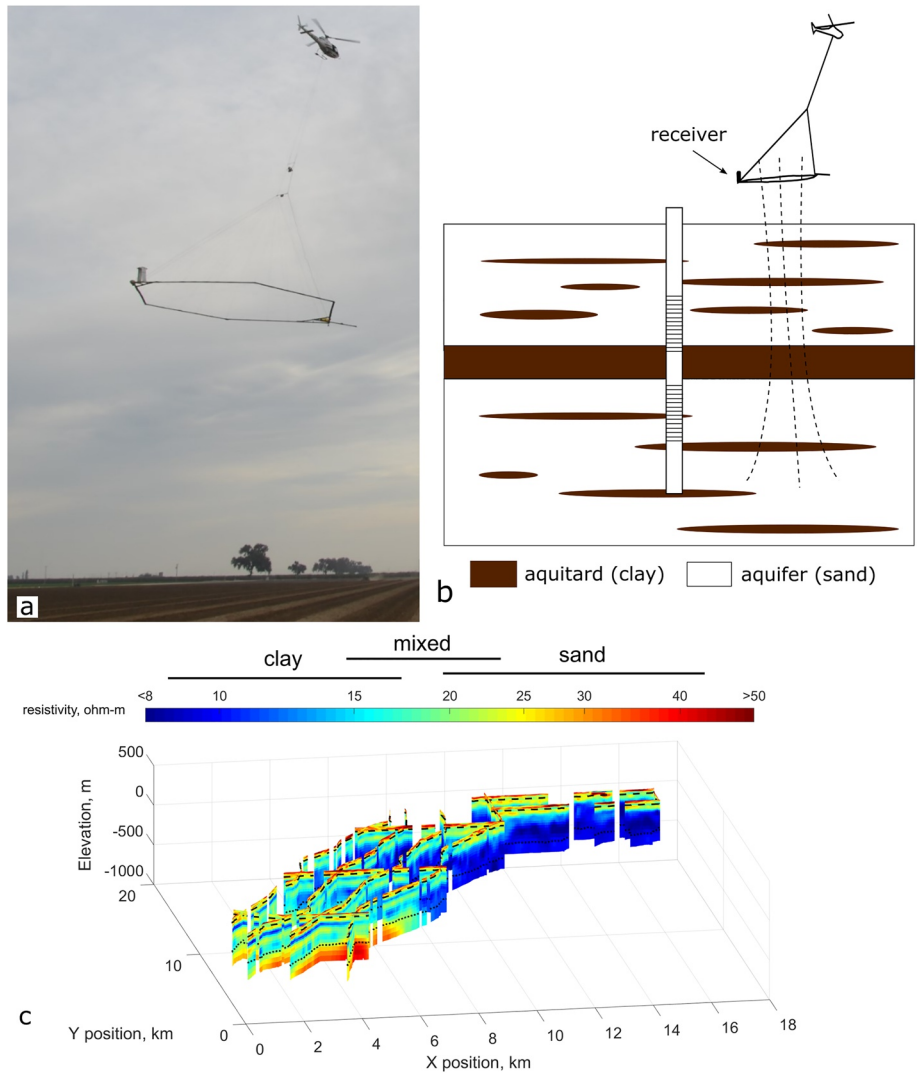

Figure 8. (a) Airborne Electromagnetic Systems (AEM) (SkyTEM) system acquiring data over the San Joaquin Valley, California, (b) Simplified schematic of AEM system, idealized magnetic fields shown as dashed lines, and (c) Inverted resistivity acquired with AEM modified from Knight et al. (2018), water table shown as a dashed line.

during acquisition, and the receiver thus measures the response of secondary electromagnetic fields as well as the magnetic field from the primary source, which is removed through processing. Frequency-domain measurements are often used with fixed-wing systems, and thus are well-equipped for surveying large areas. Their depth of investigation can range from meters to hundreds of meters. The depth of investigation is a function of the current, as well as the loop size of the transmitter and the frequencies at which the transmitter operates. Lower frequencies penetrate deeper, and higher frequencies provide more detail in the near-surface depths.

Time-domain systems generate a direct current for the source, which is rapidly shut off before the receiver starts recording for each sounding location. While this eliminates the need to remove the primary source in post-processing, it requires complex electronics. After shutting off the primary source, the receiver records the change in magnetic field with respect to time at discrete time intervals, or gates. Current popular time-domain electromagnetic systems are mounted from helicopters, so are not able to survey as quickly as fixed-wing frequency-domain systems. They do, however, have a similar depth of penetration. While the accuracy of frequency-domain systems in the shallow subsurface is limited by the frequencies selected, the accuracy of time-domain systems is limited by the shut-off time. Systems that can shut off the transmitter current more quickly are able to start recording earlier, when most of the electromagnetic signal from the near-surface (upper

~20 m) is generated. For this reason, many time-domain systems generate two soundings, a high-moment and low-moment sounding, at each location. The low-moment sounding is run at a lower current, and thus can be shut off more quickly to extract more information in the near-surface, while the high-moment sounding is run at a higher current, and while the shut-off time is slower, its signal penetrates deeper and thus it provides more information at greater depths (typically up to ~300–400 m).

Calibration and error reduction during AEM acquisition must be supported by a robust knowledge of ground elevation, signal-receiver geometry, transmitted waveforms, filter settings, and amplifier characteristics (Deszcz-Pan et al., 1998; Green & Lane, 2003). After AEM signals go through standard processing such as corrections for primary signals, height, geometry, and removal of soundings near noise sources such as power lines, an inversion process is used to estimate the conductivity of the subsurface from the raw data acquired. The inverted conductivity is acquired at dense spatial resolutions (typically on the order of 30 m between soundings, and a user-specified distance between flight lines) and moderate vertical resolutions (with layer thicknesses on the order of meters near the surface, and on the order of 10s of m at depths of 300–400 m). This data can then be converted to a 3D model of conductivity. This is often viewed either as cross-sections along line profiles, or as depth slices. Inversion models are present that vary in assumption about geologic layers or variability of conductivities at depth (Christensen et al., 2017; Siemon et al., 2009; Spies & Woodgate, 2003). Current inversion models for AEM data typically use a 1-dimensional forward model for computational efficiency, which assumes little variation in layers horizontally. This is an appropriate assumption for most sedimentary systems, where subsurface layers are fairly continuous. However, regions with sharp horizontal changes, such as heavily faulted systems, may have errors introduced from this assumption. Inversion processes are mathematically complex as several combinations of geologic layer thickness and conductivities could produce equivalent electromagnetic responses. Some inversion procedures account for this with distributions of equally probably subsurface conductivity distributions (Minsley, 2011). After producing estimates of subsurface conductivity, a lithologic model or in situ borehole data are used to develop a rock-physics transform that relates conductivity to geologic or hydrogeologic properties. This can also be used to ground-truth and choose plausible scenarios in the inversion process (Spies & Woodgate, 2003). Inversion models that relate electric resistivity to hydrostratigraphic information are described in detail by Christensen et al. (2017).

2.4. Proxy Measurements: Soil Moisture and Evapotranspiration

In the absence of, or in complement to, other means or methods for observing groundwater changes from space, the assessment of soil moisture, evaporation, or vegetation on the surface can also provide information on groundwater use (Chen & Hu, 2004; Jackson, 2002; Maxwell et al., 2007), as near-surface groundwater will directly or indirectly affect vegetation especially in arid, high infiltration (e.g., karstic systems), and irrigated regions (Hartmann et al., 2020). For instance, in an arid region, where little surface water and precipitation occur, the presence of agriculture and the associated greenness of vegetation and anomalous soil moisture provide some evidence for the use of groundwater resources. Because optical remote sensing methods are typically relatively high spatial resolution, assessment methodologies based on those observations can help to define the small, local scale activities in terms of groundwater use. However, these methods do not offer a direct measure of groundwater use, but instead an indirect means of inferring irrigation or agricultural activity that may rely on groundwater. For example, Landsat-based methods for measuring evapotranspiration could be used to constrain groundwater consumption in a region where no known surface water supply exists. In regions where water resources come from a combined portfolio of surface water and groundwater, it would be challenging to derive conclusive analysis from this approach alone.

In order to infer evapotranspiration and soil moisture from space, several techniques have been developed using visible, near-infrared, and thermal bands of Landsat and Sentinel-2. These techniques typically compare an irrigated agricultural region with an adjacent nonirrigated region to derive a change in latent heating (i.e., local cooling due to the enhanced presence of moisture) and thereby make an inference on the amount of water being evapotranspired into the atmosphere. In well-studied regions, where little known surface water is available, it would be possible to infer groundwater usage by assuming that the supply of water for evapotranspiration (ET) originates from groundwater sources. Typically, optical technologies like Landsat offer a spatial footprint of 30 m resolution, and fairly frequent sampling in time (8–15 days). The accuracy of the approaches for measuring ET depends upon the terrain, the vegetation type, the range of ET magnitude, and other confounding factors,

including the existence of a reference region to derive an ambient Bowen ratio (the ratio of latent to sensible heat flux). To further extend this approach for inference on groundwater, it would require an advanced knowledge of vegetation type and their respective ET indices, as well as a complete portfolio and proper accounting of all water sources.

Future satellite missions following the existing NASA Soil Moisture Active Passive Mission (Entekhabi et al., 2010) could provide higher resolution and longer wavelength (i.e., deeper) soil moisture observations. Current exploratory techniques using different orbits and repeat periods may offer higher sampling frequencies and resolutions closer to 3–5 km using active radar. Also, the utilization of different frequencies in the electromagnetic spectrum (e.g., P-band, 70 cm wavelength) could allow for detection of deeper signals, such as water tables several meters beneath the surface, provided the surface is dry. Also, future missions following NASA's ECOSTRESS instrument aboard the International Space Station may offer sustained evapotranspiration estimation with a sampling frequency that allows for the resolution of a diurnal cycle (i.e., two measurements daily) to better quantify the plant response to diurnal solar forcing.

3. Future Advances and Potential Directions

Here, we present future directions of the discussed methods. We focus on the three major techniques for groundwater detection: gravity measurements, InSAR, and GNSS. Figure 9 presents the spatial and temporal scales of groundwater variability and the various observational approaches. While remote sensing methods are capable of capturing groundwater dynamics on much greater spatial scales than in situ or point-based methods, distinct spatial and temporal gaps between various observational approaches still exist. Advances in other methods such as radar altimetry, lidar, and soil moisture, while not discussed, would complement other data sets to generate a coherent picture of the aquifer in question. Further, numerical groundwater models or data assimilation platforms would further serve as a valuable tool in integrating the observations to the appropriate spatiotemporal scale according to the research question.

3.1. Gravity-Based Missions

The nominal mission lifetime of GRACE-FO is 5 years, although in principle the mission could last longer depending on solar activity, as well as the overall health of the spacecraft instrumentation and subsystems. Further, the 2017 National Academy of Sciences Earth Sciences and Applications from Space Decadal Survey recommended a future mission, called Mass Change, which further advances measures of mass change within the Earth system. This points to a third mission after GRACE-FO to further continue this valuable time series of measurements. Both GRACE and GRACE-FO represent successful partnerships with the German Aerospace Center and the German Research Center for Geosciences from Germany. It is therefore likely the next mission beyond GRACE-FO will additionally leverage international partnerships. A comprehensive study of potential observing system architectures for this mission was recently concluded as part of NASA's implementation program for Mass Change (Wiese et al., 2022).

Previous studies have shown that changing the observing geometry compared to GRACE or GRACE-FO can drastically reduce the magnitude of the stripes in the gravity solution described above, and future missions could employ these improvements. Different satellite formations that sample in multiple directions, such as a “cartwheel formation” and “pendulum formation” (Elsaka et al., 2014; Wiese et al., 2009) have been proposed, and have been shown to significantly suppress the stripes, producing error patterns that are more isotropic. Further, it has been shown that two pairs of satellites (one polar pair and one lower inclined pair) have the distinct advantage of both improving the sampling geometry to get rid of stripes, while also reducing temporal aliasing errors by sampling more frequently. This can result in significant improvements in the spatial resolution and accuracy of the derived gravity fields (Wiese, Visser, & Nerem, 2011; Wiese, Visser, & Han, 2011; Wiese et al., 2012). Elsaka et al. (2014) highlights some candidate mission architectures that have been studied in the past.

A major weakness of observing groundwater using satellite gravimetry of any architecture/measurement system discussed above is the relatively coarse spatial resolution of the terrestrial water storage anomaly estimates. As the orbital height of the satellites will always fundamentally limit the spatial resolution to ∼100 km length scales (for inter-satellite ranging missions at altitudes above ∼450 km), this constraint on the data is challenging to overcome. The primary hindrance improving both the spatial and the temporal resolution of time variable gravity

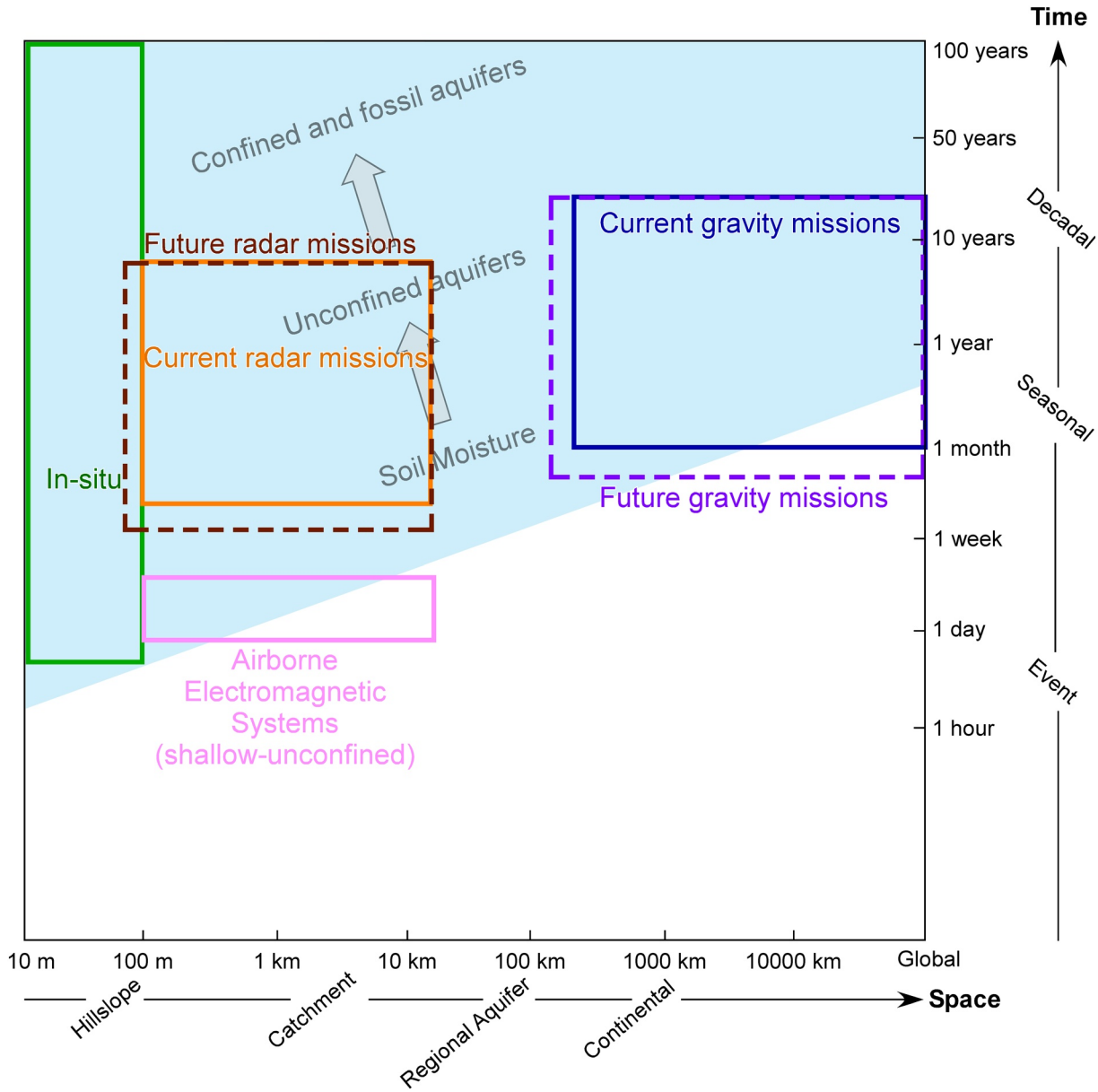

Figure 9. Spatial and temporal scales of groundwater variability and where the various observational approaches sample. Current monitoring capabilities (solid lines) and potential future capabilities (dashed lines) are indicated. Different methods and technologies can be integrated to synthesize a holistic groundwater measurement depending on the target research question.

products is the limited space-time sampling. Mass changes in the oceans and atmosphere occur on temporal scales that are too short for along-track observations of a single, polar orbiting satellite pair at ~500 km altitude to adequately observe, which introduces error into the gravity field solutions. Fortunately, groundwater typically changes over longer timescales, so that monthly data are sufficient for most applications.

Of the estimated hundreds of groundwater aquifers around the world, only GRACE was successfully able to observe approximately the largest 33 (Richey et al., 2015), and offered little information on the redistribution or consumption of water within the aquifers. The number of observable aquifers could be increased by implementing advanced observing techniques, some of which are mentioned above. Another method for addressing the coarse resolution is to combine GRACE and other observation-based data using a data assimilation approach within a land-surface model that represents groundwater explicitly (e.g., Zaitchik et al., 2008; see Section 3.5). Other

possibilities include combining GRACE data with some of the other techniques presented in this report, such as InSAR and in situ GNSS networks.

Advances in improving the temporal resolution of mass change observations requires increasing the temporal sampling via additional observations. The simplest observing system architecture to accomplish this consists of two in-line pairs of satellites, as already discussed. A constellation of small satellite pairs is additionally an appealing concept to improve the temporal sampling. Multiple pairs of satellites optimally distributed in multiple orbital planes has the potential to improve both spatial and temporal resolution of mass change fields quite substantially. However, employing the satellite-satellite tracking architecture on small satellites poses many engineering challenges in terms of required thermal and structural stability (Kornfeld et al., 2019) that still need to be understood.

Another engineering design solution to increase the spatial resolution of mass change fields is to fly the satellites in lower altitudes, thus increasing their sensitivity to short wavelength mass variations. Such a design requires some form of active drag compensation system to extend the mission lifetime to a reasonable amount. The Gravity Field and Steady-State Ocean Circulation Explorer mission utilized such technology (Floberghagen et al., 2011).

3.2. InSAR

International space agencies are investing heavily in SAR missions, making SAR a promising future method of detecting groundwater changes. The ESA has committed to the multi-decade operational Copernicus program, which comprises a minimum of two Sentinel-1 C-band SAR systems, co-flying in the same 12-day exact repeat orbit separated by 6 days. This provides land coverage at a spatial and temporal sampling density that is operationally useful for surface subsidence and uplift measurements where interferometry is possible.

The NASA-ISRO SAR (NISAR) mission will launch in the coming years and will provide global sampling every 12 days at L-band (https://nisar.jpl.nasa.gov/files/nisar/NISAR_Science_Users_Handbook1.pdf). The mission is designed for a minimum of 5 years, with optimal surface correlation properties, and is planned to satisfy sampling needs for groundwater-related subsidence measurements. Taken together with Sentinel-1, the temporal sampling can be increased further. Because groundwater changes are slow, the increased temporal sampling can help reduce errors by stacking the data from the individual satellites (Note: Sentinel and NISAR cannot be stacked together), or in model inversion. These two systems have dense spatial and temporal coverage, and the data are (for Sentinel-1) or will be (for NISAR) freely and openly available in the NASA SAR archives at the Alaska Satellite Facility. Together, they provide an operational data set for the groundwater application that is sufficient for most purposes.

The commercial SAR market is also actively growing. Many start-up companies are designing and building small SAR constellations to feed commercial remote sensing monitoring needs. Generally, the target customers require fast revisit (1 day or less) and fine resolution. As a result, most of the commercial SAR satellites have fine resolution, narrow swaths (~20 km), limited on-orbit duty cycles, and operate in bands (such as X-band) that have sufficient bandwidth to support fine resolution. As such, they are not optimally configured to map wide areas with a consistent interferometric sampling strategy to develop dense stacks of data for tracking deformation. As the typical region of interest for studying aquifers is of order 100 × 200 km, commercial SAR tends to have swaths that are too narrow. New small-SAT SAR solutions arising in the commercial sector would be expected to have even narrower swaths, requiring a greater number of satellites for a sufficient sampling strategy for aquifers. Nonetheless, apart from spatial scale challenges, the intrinsic resolutions and accuracies of civil and commercial SAR systems are adequate for all measurements needed for assessing changes in the aquifer over time.

3.3. GNSS

Generally, GNSS networks are densifying over time. For many regions of the world such as the United States, Europe, and Japan, networks are dense enough to view the earth as being globally imaged by GNSS, as in Figure 10 derived from a GNSS Mega-network (Hammond et al., 2021). Advances in GNSS receiver technologies also carry important implications for the future. Geodetic-quality receivers are increasingly cost effective, compact, and power friendly: some roughly the size of a credit card and drawing 1 W or less of power (such as the AsteRx-m3 Pro, EMEA, Belgium). The cost and size of individual parts, such as receivers, antennas, and solar

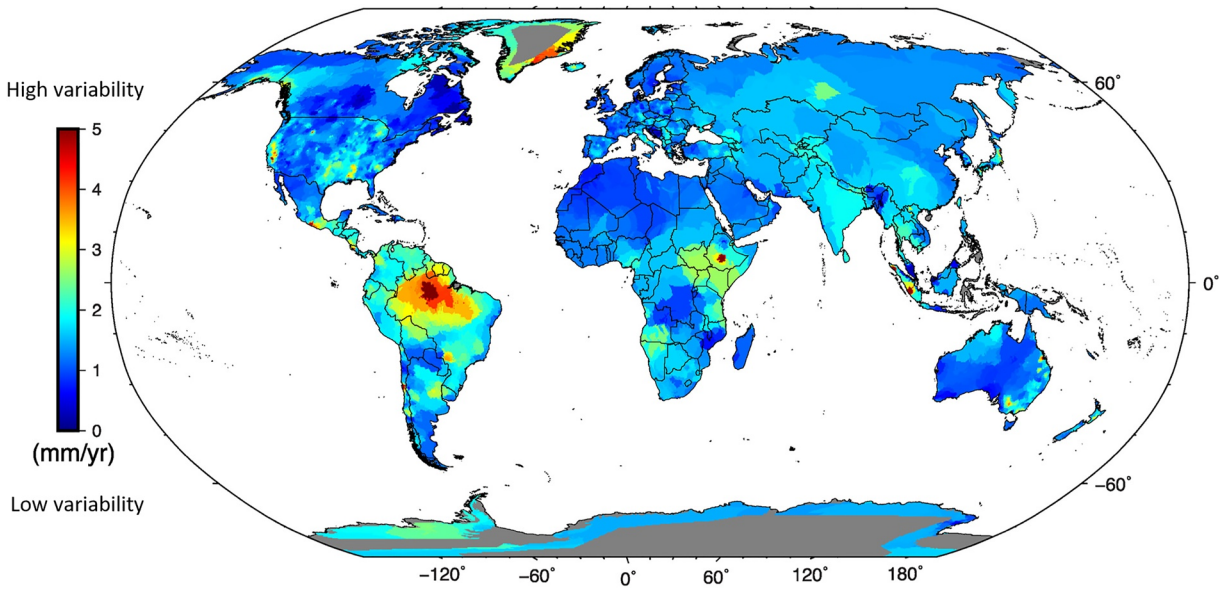

Figure 10. (After Hammond et al., 2021). Variability of nonseasonal vertical land motion based on the global Global Navigational Satellite System (GNSS) mega-network. Big interannual variations in vertical displacement in the Amazon River basin may reflect solid Earth's elastic response to water loss during periods of drought (or low precipitation) and water gain during years of heavy precipitation.

panels, are increasingly becoming compact, which allows for ease of strategic deployment. With this continued growth of the global GNSS network, groundwater monitoring and its associated surface responses (elastic/inelastic subsidence, tectonic uplift from unburdening) using GNSS will become more robust.

3.4. Integration of Different Remote Sensing Data Sets

The techniques presented above vary in spatial and temporal scales, making the individual techniques only suitable for a certain range of spatiotemporal assessments. Combining various remote sensing approaches therefore greatly enhances the applicability of the presented techniques. In particular, synthesizing surface deformation data sets with other approaches provides a means to understand geologic response associated with groundwater changes and allows for better uncertainty quantification.

California's Central Valley, briefly discussed in previous sections, is a stellar example of how combining various remote sensing approaches provide a holistic picture of regional hydrology and geology. GRACE (and GRACE-FO thereafter) have measured a steady decline of groundwater levels in California (Famiglietti et al., 2011; Scanlon et al., 2012). There has also been continued subsidence recorded within the Central Valley, from InSAR and continuous GNSS measurements (Amos et al., 2014; Faunt et al., 2016; Poland et al., 1975; Sneed & Brandt, 2015). While gravity and surface-deformation approaches have been, respectively, validated against well data and extensometers, the large spatial scale of GRACE/GRACE-FO products and the complex geologic heterogeneity driving a nonlinear surface response pose limits in the standalone use of individual techniques. Recent efforts by Liu et al. (2019) and Vasco et al. (2022) closed this gap by correlating GRACE-measured basin-scale groundwater depletion trends to subsidence patterns from Sentinel-1. Kim et al. (2021) compared groundwater depletion and subsidence trends at a sub-basin scale for the first time using 12.5-km resolution downscaled-GRACE/GRACE-FO (see following section), well data, Sentinel-1, and GNSS. This displayed the differences in magnitude and temporal lag between groundwater depletion and recorded subsidence by different sub-basins. Recent water balance approach by Ahamed et al. (2022) displayed that integration of various remote sensing data can successfully estimate and monitor groundwater storage changes across spatial scales finer than GRACE. Such efforts to integrate various remote sensing data set. allow us to understand the dynamic spatiotemporal relationship between groundwater storage and elastic/inelastic geologic response.

3.5. Numerical Modeling

Numerical models can be an important tool for relating remotely sensed observations to groundwater properties or conditions of interest (Kumar et al., 2006; Rodell et al., 2004). For example, InSAR and GNSS data sets provide estimates of surface deformation, which is primarily a function of pore pressure change in clays. While this is related to groundwater flow in aquifers, the relationship is complex and nonlinear, particularly during inelastic deformation. For this reason, relating deformation measurements to groundwater systems empirically is often not feasible. In these cases, modeling the physical mechanisms for deformation can provide additional information about aquifer system response to groundwater withdrawals or recharge. Similarly, GRACE data provide an estimate of total water storage change, but typically require a robust model to be disaggregated into groundwater, soil moisture, snow water equivalent, and surface water components or to be downscaled to finer resolutions. Models that are capable of integrating multiple remote sensing data sets, as well as in situ data, at scales that are relevant to water management, are thus critical for advancing our ability to use remotely sensed data for groundwater evaluation.

To first order, models provide estimates of the variable of interest, using known physics, which can be valuable for testing hypotheses or scenarios in which observations are inadequate or impossible. At best, models provide a framework to fill measurement gaps and can be used in conjunction with observations to achieve better results in terms of sampling, resolution, or accuracy. Numerical groundwater storage and flow simulations exist over a variety of domains and resolutions, and for a variety of purposes. As a model is always a discretized and idealized representation of reality, decisions regarding the realism and complexity of simulated hydrogeological processes depends on the application and the available computer resources. For instance, model physics that would be employed to understand lateral groundwater flow through porous media at meter-scale resolution would differ significantly from those that would be employed to represent gross groundwater storage changes at regional to continental scales (100–1,000 km resolution).

Existing groundwater models can represent soil physics at local scales relevant to water management using, for example, the Richards equation to describe pressure driven lateral and vertical flow through a variably saturated soil column. These models require high-resolution discretization (<1 km) in order for the physics to be appropriate. Because those models are typically operated over smaller domains, they are typically less relevant to large scale observations (such as those from space-borne gravity or GNSS networks), and more appropriate for local-scale observations such as in situ well observations and InSAR. Therefore, in situ data such as wells and hydrogeologic parameters are often used in the calibration of groundwater models. For instance, the ParFlow model (Kollet & Maxwell, 2006), applies Richards' equation for variably saturated 3D subsurface flow and shallow water equations for surface flow. This is a modular, coupled land model that represents the full energy budget, vegetative and snow processes and applies robust nonlinear solvers and efficient multigrid linear solvers allowing parallel implementation using multiple approaches and architectures. This makes the model applicable to a wide range of hydrology problems and basins, from small catchments to continent scales if sufficient computational resources are available (e.g., Maxwell et al., 2015). ParFlow is advantageous for integrating surface and groundwater models, but does not have the ability to simulate surface deformation, limiting its applicability to integrating InSAR or GNSS data sets.

MODFLOW from the U.S. Geological Survey is a finite-difference flow model that is also suited for small- to regional-scale aquifers. The code has been modified to fit various cases, such as SEAWAT for variable-density flow, and MODFLOW-OHWM for conjunctive use of surface water and groundwater. FEFLOW, SUTRA, and HydroGeoSphere are different types of well-used groundwater models. A current frontier in groundwater modeling research is to apply very high-resolution models to a large study domain, such as the continental United States, though these simulations can suffer from a lack of relevant groundwater observations for calibration/validation.

For larger-scale models (i.e., grid resolutions 12.5 km or coarser), groundwater representations are more empirical, representing the subsurface water storage using a bucket model, or a series of buckets. These models do not represent lateral subsurface flows, but treat each model grid cell as a separate 1-dimensional control volume with no lateral communication. Such models are typically sufficient for coupling to atmospheric models in global climate simulations or for representing regional-scale hydrology. For large-scale hydrology and land-surface models, data assimilation can be a useful means to perform parameter calibration or state estimation. An example of a successful model implementation using the GRACE data has been in the numerical assimilation of monthly

GRACE observations into a 12.5 km land-surface model (the Catchment Land Surface Model), in pursuit of higher spatial and temporal resolution information on terrestrial water storage and its components (Girotto et al., 2017; Houborg et al., 2012; Kumar et al., 2016; Li et al., 2019; Zaitchik et al., 2008). The model disaggregates the lumped terrestrial water storage variable into canopy water, snow water, surface soil moisture, root zone soil moisture, and shallow groundwater. The disaggregation and downscaling allow for a better understanding of water storage evolution in time and space. The results are used as an input to the U.S. Drought Monitor (Houborg et al., 2012) and also show promise in contributing to flood forecasting (Reager et al., 2015).

As high-performance computing allows for faster processing and parallelization of discretized physical models, the ability to harness that computing power for numerical model simulations will grow in response. It will then be possible to include more explicit physical representations of subsurface processes in model studies over larger domains. These physics should provide a more complete picture of groundwater variations and flows for a study region and better context for both in situ and remotely sensed observations. Fully coupled Earth system models have gained recent attention as research has revealed interdependencies between water and energy processes in the subsurface, on the land surface, and in the lower atmosphere. For example, PF.WRF (Maxwell et al., 2011) couples the Weather Research and Forecasting atmospheric model with a parallel hydrology model (ParFlow) that fully integrates three-dimensional, variably saturated subsurface flow with overland flow.

Surface deformation measurements provide valuable hydrologic information, but are challenging to relate to aquifer system dynamics due to the nonlinear relationship between groundwater levels and deformation. The mechanism for deformation is well-studied, and can be simulated as a function of aquifer water levels. Models relating deformation to water levels have been implemented with extensometer, GNSS and InSAR data (Alghamdi et al., 2020; Helm, 1975; Hoffmann et al., 2003; Smith & Li, 2021). In addition, most MODFLOW-based codes have a built-in subsidence package (SUB) that simulates elastic and inelastic deformation, as well as the resulting flux from fine-grained layers into aquifer systems that occurs (Hoffmann et al., 2003). There are also a number of poro-elastic models that consider 3D deformation of aquifer systems (Boni et al., 2020), although these typically do not consider inelastic deformation.

While some models exist to simulate deformation, the vast majority of groundwater models, and virtually all coupled groundwater-surface water models, do not have the ability to simulate deformation. This is significant, because in confined aquifers, deformation represents a substantial flux from fine-grained layers into the principal aquifer system (Faunt et al., 2009), and could introduce model bias if unaccounted for. The combination of hydrological models with deformation models will likely be explored in the next decade, so that measurements of hydrological change (from GRACE, well observations, etc.) and surface deformation (from InSAR or GNSS) can be directly ingested into the same numerical framework. Such simultaneous ingestion of multiple independent data sources could offer more comprehensive insights on the multi-disciplinary processes involved in groundwater change, for example, enabling the spatial downscaling of satellite gravimetry-based water storage information using high resolution InSAR observations of land surface subsidence and elastic rebound.

4. Summary and Conclusions

Groundwater is a critical resource, and its importance will only continue to increase with climate change and population growth. Water is the major pathway in which global residents will experience climate change—through extreme climate events (droughts and floods), decreased supply, and increased water quality issues (e.g., rising salinities, arsenic release from pumping, and pathogen increase from heat). As surface water becomes more erratically available, groundwater will be a key resource to understand and manage to ensure global water security. Freshwater is heterogeneously distributed around Earth and the interactions between different water storage areas (surface water, atmospheric water, groundwater, glaciers, etc.) are complex. Therefore, it is important to consider groundwater as a unique entity in quantification and management, rather than as part of a lump sum water budget (Gleeson et al., 2020). Many of the United Nation's Sustainable Development Goals (e.g., zero hunger, good health and well-being, clean water and sanitation, climate action, and life below water and on land) directly or indirectly involve groundwater, highlighting groundwater as a cross-cutting resource crucial to future challenges (e.g., 21st Century Grand Challenges as presented by the National Councils; NASEM, 2019).

While well-managed in situ observation networks with dense spatiotemporal sampling are superior to the coarse-resolution measurements provided by remote sensing, such networks can be cost-prohibitive, labor

intensive to maintain, and are increasingly difficult to find around the world (Stokstad, 1999). Conflicting political interests around international water bodies may also render in situ data difficult to obtain. Within this context, recent advances in remote sensing provide a means to monitor groundwater and related geophysical changes at spatial scales otherwise unattainable with in situ methods (Famiglietti et al., 2015). These advances also ease data distribution, inviting a range of users to utilize the data according to their needs. This is being augmented by open, community-based coding programs such as Python or Google Earth Engine that allow users to share codes to manipulate data sets.

Several remote sensing, space-based techniques have been presented in this review. Although groundwater storage change can be monitored with gravity- and deformation-based measurements, each have limitations. The primary limitation of gravity-based measurements is resolution, while the primary limitation of deformation-based measurements is the lower sensitivity in unconfined aquifers, though they are often the first source of extracted groundwater resources. Methods to address these limitations could greatly advance the ability of remote sensing to estimate groundwater storage change at a resolution that is applicable for water management in management districts, which often are smaller in area than the resolution of gravity-based measurements.

In arid regions with minimal surface water, soil moisture, and evapotranspiration can be used to infer groundwater usage, assuming groundwater is the sole or major water source. AEM systems are capable of mapping available groundwater, aquifer heterogeneity, and the presence of fresh and saline groundwater. Individual methods have varying spatial, temporal, and technological limits, which make them appropriate for different regions and research goals. In this light, numerical models can serve as a valuable tool to integrate the various data sets and simulate groundwater processes, and the continued development of models that can integrate multiple remote sensing data sets is an area of great promise for improved groundwater resource evaluation. In certain cases, such as groundwater quality, where close contact with the porewater or aquifer medium is required, strategic deployment of in situ data may outweigh the benefits of remote sensing. In cases where continuity of data is critical, the gaps in remote sensing data due to mission termination or technological shifts may adversely impact outcomes. Nonetheless, remote sensing methods provide "big picture" assessments of groundwater globally, and lead the technological vanguard toward groundwater sustainability. Future advances in remote sensing, in addition to better data assimilation methods, will greatly enhance our ability to monitor and quantify global groundwater resources in the long-term.

Data Availability Statement

No new data were generated for this review paper.

Acknowledgments
The research was carried out at the Jet Propulsion Laboratory, California Institute of Technology, under a contract with the National Aeronautics and Space Administration (80NM0018D0004). A portion of this research was supported by NASA ROSES Applied Sciences Water Resources Program and the NASA GRACE/GRACE-FO science team.

References

Abdalati, W., Zwally, H. J., Bindschadler, R., Csatho, B., Farrell, S. L., Fricker, H. A., et al. (2010). The ICESat-2 laser altimetry mission. *Proceedings of the IEEE*, *98*(5), 735–751. https://doi.org/10.1109/jproc.2009.2034765

Abraham, J. D., & Cannia, J. C. (2011). Airborne electromagnetic surveys for 3d geological mapping. *USGS Staff*, *506*. Retrieved from https://digitalcommons.unl.edu/usgsstaffpub/506

Ahamed, A., Knight, R., Alam, S., Pauloo, R., & Melton, F. (2022). Assessing the utility of remote sensing data to accurately estimate changes in groundwater storage. *Science of The Total Environment*, *807*, 150635.

Alghamdi, A., Hesse, M. A., Chen, J., & Ghattas, O. (2020). Bayesian poroelastic aquifer characterization from InSAR surface deformation data. Part I: Maximum a posteriori estimate. *Water Resources Research*, *56*(10), e2020WR027391. https://doi.org/10.1029/2020wr027391

Alley, W. M., Healy, R. W., LaBaugh, J. W., & Reilly, T. E. (2002). Flow and storage in groundwater systems. *Science*, *296*(5575), 1985–1990. https://doi.org/10.1126/science.1067123

Amelung, F., Galloway, D. L., Bell, J. W., Zebker, H. A., & Laczniak, R. J. (1999). Sensing the ups and downs of Las Vegas: InSAR reveals structural control of land subsidence and aquifer-system deformation. *Geology*, *27*(6), 483–486. https://doi.org/10.1130/0091-7613(1999)027%3C0483:STUADO%3E2.3.CO;2

Amos, C. B., Audet, P., Hammond, W. C., Bürgmann, R., Johanson, I. A., & Blewitt, G. (2014). Uplift and seismicity driven by groundwater depletion in central California. *Nature*, *509*(7501), 483–486. https://doi.org/10.1038/nature13275

An, K. (2015). *Investigating the relationship between land subsidence and groundwater depletion in the north China plain using GRACE and ICESat* (Doctoral dissertation) UCLA. Retrieved from https://escholarship.org/uc/item/60931454

Argus, D. F., Fu, Y., & Landerer, F. W. (2014). Seasonal variation in total water storage in California inferred from GPS observations of vertical land motion. *Geophysical Research Letters*, *41*(6), 1971–1980. https://doi.org/10.1002/2014GL059570

Argus, D. F., Heflin, M. B., Peltzer, G., Webb, F. H., & Crampe, F. (2005). Interseismic strain accumulation and anthropogenic motion in metropolitan Los Angeles. *Journal of Geophysical Research*, *101*(B4), B04401. https://doi.org/10.1029/2003JB002934

Argus, D. F., Landerer, F. W., Wiese, D. N., Martens, H. R., Fu, Y., Famiglietti, J. S., et al. (2017). Sustained water loss in California's mountain ranges during severe drought from 2012 to 2015 inferred from GPS. *Journal of Geophysical Research: Solid Earth*, *122*(12), 10–559. https://doi.org/10.1002/2017JB014424

Arola, T., Okkonen, J., & Jokisalo, J. (2016). Groundwater utilisation for energy production in the nordic environment: An energy simulation and hydrogeological modelling approach. *Journal of Water Resource and Protection*, *8*(06), 642–656. https://doi.org/10.4236/jwarp.2016.86053

Ball, L. B., Davis, T. A., Minsley, B. J., Gillespie, J. M., & Landon, M. K. (2020). Probabilistic categorical groundwater salinity mapping from airborne electromagnetic data adjacent to California's Lost Hills and Belridge oil fields. *Water Resources Research*, *56*(6), e2019WR026273. https://doi.org/10.1029/2019wr026273

Baudouin, P., Durozoy, G., & Utard, M. (1967). Etude par prospection électromagnétic aérienne d'un contact eau douce eau salée dans le delta du Rhône. Mining and Groundwater Geophysics 1967. *Report Geological Survey of Canada*, *26*, 626–637.

Bawden, G. W., Thatcher, W., Stein, R. S., Hudnut, K. W., & Peltzer, G. (2001). Tectonic contraction across Los Angeles after removal of groundwater pumping effects. *Nature*, *412*(6849), 812–815. https://doi.org/10.1038/35090558

Becker, M. W. (2006). Potential for satellite remote sensing of ground water. *Groundwater*, *44*(2), 306–318. https://doi.org/10.1111/j.1745-6584.2005.00123.x

Berg, S. J., & Illman, W. A. (2011). Capturing aquifer heterogeneity: Comparison of approaches through controlled sandbox experiments. *Water Resources Research*, *47*(9). https://doi.org/10.1029/2011WR010429

Bertiger, W., Bar-Sever, Y., Dorsey, A., Haines, B., Harvey, N., Hemberger, D., et al. (2020). GipsyX/RTGx, a new tool set for space geodetic operations and research. *Advances in Space Research*, *66*(3), 469–489. https://doi.org/10.1016/j.asr.2020.04.015

Blewitt, G., Hammond, W. C., & Kreemer, C. (2018). Harnessing the GPS data explosion for interdisciplinary science. *Eos*, *99*, 1–2. https://doi.org/10.1029/2018eo104623

Boni, R., Meisina, C., Teatini, P., Zucca, F., Zoccarato, C., Franceschini, A., et al. (2020). 3D groundwater flow and deformation modelling of Madrid aquifer. *Journal of Hydrology*.

Borsa, A. A., Agnew, D. C., & Cayan, D. R. (2014). Ongoing drought-induced uplift of the Western United States. *Science*, *345*(6204), 1587–1590. https://doi.org/10.1126/science.1260279

Bürgmann, R., Hilley, G., Ferretti, A., & Novali, F. (2006). Resolving vertical tectonics in the San Francisco Bay Area from permanent scatterer InSAR and GPS analysis. *Geology*, *34*(3), 221–224. https://doi.org/10.1130/G22064.1

Calderhead, A. I., Martel, R., Alasset, P. J., Rivera, A., & Garfias, J. (2009). Land subsidence induced by groundwater pumping monitored by C-band D-InSAR and field data in the Toluca Valley Mexico. *International Journal of Remote Sensing*, *36*(1), 9–23. https://doi.org/10.5589/m10-024

Castellazzi, P., Martel, R., Galloway, D. L., Longuevergne, L., & Rivera, A. (2016). Assessing groundwater depletion and dynamics using GRACE and InSAR: Potential and limitations. *Groundwater*, *54*(6), 768–780. https://doi.org/10.1111/gwat.12453

Chapelle, F. (1997). *The hidden sea: Ground water, springs, and wells*. GeoScience Press.

Chatterjee, R. S., Fruneau, B., Rudant, J. P., Roy, P. S., Frison, P. L., Lakhera, R. C., et al. (2006). Subsidence of Kolkata (Calcutta) City, India during the 1990s as observed from space by differential synthetic aperture radar interferometry (D-InSAR) technique. *Remote Sensing of Environment*, *102*(1–2), 176–185. https://doi.org/10.1016/j.rse.2006.02.006

Chaussard, E., Amelung, F., Abidin, H., & Hong, S. H. (2013). Sinking cities in Indonesia: ALOS PALSAR detects rapid subsidence due to groundwater and gas extraction. *Remote Sensing of Environment*, *128*, 150–161. https://doi.org/10.1016/j.rse.2012.10.015

Chaussard, E., Wdowinski, S., Cabral-Cano, E., & Amelung, F. (2014). Land subsidence in central Mexico detected by ALOS InSAR time-series. *Remote Sensing of Environment*, *140*, 94–106. https://doi.org/10.1016/j.rse.2013.08.038

Chen, F., Lin, H., Zhang, Y., & Lu, Z. (2012). Ground subsidence geo-hazards induced by rapid urbanization: Implications from InSAR observation and geological analysis. *Natural Hazards and Earth System Sciences*, *12*(4), 935–942. https://doi.org/10.5194/nhess-12-935-2012

Chen, J., Knight, R., & Zebker, H. A. (2017). The temporal and spatial variability of the confined aquifer head and storage properties in the San Luis Valley, Colorado inferred from multiple InSAR missions. *Water Resources Research*, *53*(11), 9708–9720. https://doi.org/10.1002/2017WR020881

Chen, X., & Hu, Q. (2004). Groundwater influences on soil moisture and surface evaporation. *Journal of Hydrology*, *297*(1–4), 285–300. https://doi.org/10.1016/j.jhydrol.2004.04.019

Christensen, N. K., Minsley, B. J., & Christensen, S. (2017). Generation of 3-D hydrostratigraphic zones from dense airborne electromagnetic data to assess groundwater model prediction error. *Water Resources Research*, *53*(2), 1019–1038. https://doi.org/10.1002/2016WR019141

Collett, L. S. (1967). Resistivity mapping by electromagnetic methods. Mining and Groundwater Geophysics 1967. *Report Geological Survey of Canada*, *26*, 615–624.

Cresswell, R. G., Dent, D. L., Jones, G. L., & Galloway, D. S. (2004). Three-dimensional mapping of salt stores in the southeast Murray–Darling Basin, Australia. *Soil Use & Management*, *20*(2), 133–143. https://doi.org/10.1111/j.1475-2743.2004.tb00348.x

Dehghan-Soraki, Y., Sharifikia, M., & Sahebi, M. R. (2015). A comprehensive interferometric process for monitoring land deformation using ASAR and PALSAR satellite interferometric data. *GIScience and Remote Sensing*, *52*(1), 58–77. https://doi.org/10.1080/15481603.2014.989774

Deszcz-Pan, M., Fitterman, D. V., & Labson, V. F. (1998). Reduction of inversion errors in helicopter EM data using auxiliary information. *Exploration Geophysics*, *29*(2), 142–146. https://doi.org/10.1071/EG998142

Dewar, N., & Knight, R. (2020). Estimation of the top of the saturated zone from airborne electromagnetic data. *Geophysics*, *85*(5), EN63–EN76. https://doi.org/10.1190/geo2019-0539.1

Dickinson, J. S., Buik, N., Matthews, M. C., & Snijders, A. (2009). Aquifer thermal energy storage: Theoretical and operational analysis. *Géotechnique*, *59*(3), 249–260. https://doi.org/10.1680/geot.2009.59.3.249

Döll, P. (2009). Vulnerability to the impact of climate change on renewable groundwater resources: A global-scale assessment. *Environmental Research Letters*, *4*(3), 035006. https://doi.org/10.1088/1748-9326/4/3/035006

Donnellan, A., Zebker, H., & Ranson, K. J. (2008). Radar and lidar measurement of terrestrial processes. *Eos*, *89*(38), 349–350. https://doi.org/10.1029/2008EO380002

Earman, S., & Dettinger, M. (2011). Potential impacts of climate change on groundwater resources–a global review. *Journal of Water and Climate Change*, *2*(4), 213–229. https://doi.org/10.2166/wcc.2011.034

Eckstein, G. (2005). Protecting a hidden treasure: The U.N. International law commission and the international law of transboundary ground water resources. In *Am. Univ. Sustain. Dev. Law policy 5* (pp. 5–12).

Edmunds, W. M. (2004). Silent springs: Groundwater resources under threat. In *Managing water resources, past and present* (pp. 13–34). Oxford University Press.

Elsaka, B., Raimondo, J. C., Brieden, P., Reubelt, T., Kusche, J., Flechtner, F., et al. (2014). Comparing seven candidate mission configurations for temporal gravity field retrieval through full-scale numerical simulation. *Journal of Geodesy*, *88*(1), 31–43. https://doi.org/10.1007/s00190-013-0665-9

Entekhabi, D., Njoku, E. G., O'Neill, P. E., Kellogg, K. H., Crow, W. T., Edelstein, W. N., et al. (2010). The soil moisture active passive (SMAP) mission. *Proceedings of the IEEE*, *98*(5), 704–716. https://doi.org/10.1109/JPROC.2010.2043918

Enzminger, T. L., Small, E. E., & Borsa, A. A. (2019). Subsurface water dominates Sierra Nevada seasonal hydrologic storage. *Geophysical Research Letters*, *46*(21), 11993–12001. https://doi.org/10.1029/2019GL084589

Eppler, J., & Rabus, B. (2012). Monitoring urban infrastructure with an adaptive multilooking InSAR technique. *ESASP*, *697*, 68. http://articles.adsabs.harvard.edu/pdf/2012ESASP.697E.68E

Erban, L. E., Gorelick, S. M., & Zebker, H. A. (2014). Groundwater extraction, land subsidence, and sea-level rise in the Mekong Delta, Vietnam. *Environmental Research Letters*, *9*(8), 084010. https://doi.org/10.1088/1748-9326/9/8/084010

Famiglietti, J. S. (2014). The global groundwater crisis. *Nature Climate Change*, *4*(11), 945–948. https://doi.org/10.1038/nclimate2425

Famiglietti, J. S. (2019). A map of the future of water, Trend. Retrieved from https://www.pewtrusts.org/en/trend/archive/spring-2019/a-map-of-the-future-of-water

Famiglietti, J. S., Cazenave, A., Eicker, A., Reager, J. T., Rodell, M., & Velicogna, I. (2015). Satellites provide the big picture. *Science*, *349*(6249), 684–685. https://doi.org/10.1126/science.aac9238

Famiglietti, J. S., Lo, M., Ho, S. L., Bethune, J., Anderson, K. J., Syed, T. H., et al. (2011). Satellites measure recent rates of groundwater depletion in California's Central Valley. *Geophysical Research Letters*, *38*(3), 2010GL046442. https://doi.org/10.1029/2010GL046442

FAO (Food and Agriculture Organization), Burchi, S., & Mechlem, K. (2005). *Groundwater in international law: Compilation of treaties and other legal instruments (No. 86)*. Food and Agriculture Organization. Retrieved from http://www.fao.org/3/y5739e/y5739e00.pdf

Farber, E., Vengosh, A., Gavrieli, I., Marie, A., Bullen, T. D., Mayer, B., et al. (2004). The origin and mechanisms of salinization of the Lower Jordan River. *Geochimica et Cosmochimica Acta*, *68*(9), 1989–2006. https://doi.org/10.1016/j.gca.2003.09.021

Farr, T. G., & Liu, Z. (2015). Monitoring subsidence associated with groundwater dynamics in the Central Valley of California using interferometric radar. *Remote Sensing of the Terrestrial Water Cycle*, *206*, 397–406. https://doi.org/10.1002/9781118872086.ch24

Faunt, C. C. (2009). Groundwater availability of the Central Valley aquifer, California. *U. S. Geological Survey Professional Paper*, *1766*. https://pubs.usgs.gov/pp/1766/

Faunt, C. C., Hanson, R. T., Belitz, K., Schmid, W., Predmore, S. P., Rewis, D. L., & McPherson, K. (2009). Groundwater availability of the Central Valley aquifer, California. *U. S. Geological Survey Professional Paper*, *1776*, 225.

Faunt, C. C., Sneed, M., Traum, J., & Brandt, J. T. (2016). Water availability and land subsidence in the Central Valley, California, USA. *Hydrogeology Journal*, *24*(3), 675–684. https://doi.org/10.1007/s10040-015-1339-x

Ferguson, G., & Gleeson, T. (2012). Vulnerability of coastal aquifers to groundwater use and climate change. *Nature Climate Change*, *2*(5), 342–345. https://doi.org/10.1038/nclimate1413

Ferretti, A., Savio, G., Barzaghi, R., Borghi, A., Musazzi, S., Novali, F., et al. (2007). 2007. Submillimeter accuracy of InSAR time series: Experimental validation. *IEEE Transactions on Geoscience and Remote Sensing*, *45*(5), 1142–1153. https://doi.org/10.1109/TGRS.2007.894440

Fetter, C. W. (2001). *Applied hydrogeology*. NJ. Prentice Hall Publishing.

Fitterman, D. V., & Deszcz-Pan, M. (1998). Helicopter EM mapping of saltwater intrusion in everglades national park, Florida. *Exploration Geophysics*, *29*(1–2), 240–243. https://doi.org/10.1071/EG998240

Floberghagen, R., Fehringer, M., Lamarre, D., Muzi, D., Frommknecht, B., Steiger, C., et al. (2011). Mission design, operation and exploitation of the gravity field and steady-state ocean circulation explorer mission. *Journal of Geodesy*, *85*(11), 749–758. https://doi.org/10.1007/s00190-011-0498-3

Fricker, H. A., Borsa, A., Minster, B., Carabajal, C., Quinn, K., & Bills, B. (2005). Assessment of ICESat performance at the salar de Uyuni, Bolivia. *Geophysical Research Letters*, *32*(21), L21S06. https://doi.org/10.1029/2005GL023423

Gabriel, A. K., Goldstein, R. M., & Zebker, H. A. (1989). Mapping small elevation changes over large areas: Differential radar interferometry. *Journal of Geophysical Research*, *94*(B7), 9183–9191. https://doi.org/10.1029/JB094iB07p09183

Galloway, D. L., & Burbey, T. J. (2011). Regional land subsidence accompanying groundwater extraction. *Hydrogeology Journal*, *19*(8), 1459–1486. https://doi.org/10.1007/s10040-011-0775-5

Galloway, D. L., Hudnut, K. W., Ingebritsen, S. E., Phillips, S. P., Peltzer, G., Rogez, F., & Rosen, P. A. (1998). InSAR detection of aquifer system compaction and land subsidence, Antelope Valley, Mojave Desert, California. *Water Resources Research*, *34*(10), 2573–1585. https://doi.org/10.1029/98wr01285

Getirana, A., Kumar, S., Girotto, M., & Rodell, M. (2017). Rivers and floodplains as key components of global terrestrial water storage variability. *Geophysical Research Letters*, *44*(20), 10359–10368. https://doi.org/10.1002/2017GL074684

Giordano, M. (2009). Global groundwater? Issues and solutions. *Annual Review of Environment and Resources*, *34*(1), 153–178. https://doi.org/10.1146/annurev.environ.030308.100251

Girotto, M., De Lannoy, G. J., Reichle, R. H., Rodell, M., Draper, C., Bhanja, S. N., & Mukherjee, A. (2017). Benefits and pitfalls of GRACE data assimilation: A case study of terrestrial water storage depletion in India. *Geophysical Research Letters*, *44*(9), 4107–4115. https://doi.org/10.1002/2017GL072994

Gleeson, T., Smith, L., Moosdorf, N., Hartmann, J., Dürr, H. H., Manning, A. H., et al. (2011). Mapping permeability over the surface of the Earth. *Geophysical Research Letters*, *38*(2). https://doi.org/10.1029/2010GL045565

Gleeson, T., Villholth, K., Taylor, R., Perrone, D., & Hyndman, D. (2019). Groundwater: A call to action. *Nature*, *576*(7786), 213. https://doi.org/10.1038/d41586-019-03711-0

Gleeson, T., Wada, Y., Bierkens, M. F., & Van Beek, L. P. (2012). Water balance of global aquifers revealed by groundwater footprint. *Nature*, *488*(7410), 197–200. https://doi.org/10.1038/nature11295

Gleeson, T., Wang-Erlandsson, L., Zipper, S. C., Porkka, M., Jaramillo, F., Gerten, D., et al. (2020). The water planetary boundary: Interrogation and revision. *One Earth*, *2*(3), 223–234. https://doi.org/10.1016/j.oneear.2020.02.009

Goebel, M., Knight, R., & Halkjær, M. (2019). Mapping saltwater intrusion with an airborne electromagnetic method in the offshore coastal environment, Monterey Bay, California. *Journal of Hydrology: Regional Studies*, *23*, 100602. https://doi.org/10.1016/j.ejrh.2019.100602

Goldstein, R. M., Zebker, H. A., & Werner, C. L. (1988). Satellite radar interferometry: Two-dimensional phase unwrapping. *Radio Science*, *23*(4), 713–720. https://doi.org/10.1029/rs023i004p00713

Gottschalk, I., Knight, R., Asch, T., Abraham, J., & Cannia, J. (2020). Using an airborne electromagnetic method to map saltwater intrusion in the northern Salinas Valley, California. *Geophysics*, *85*(4), B119–B131. https://doi.org/10.1190/geo2019-0272.1

Gourmelen, N., Kim, S. W., Shepherd, A., Park, J. W., Sundal, A. V., Björnsson, H., & Pálsson, F. (2011). Ice velocity determined using conventional and multiple-aperture InSAR. *Earth and Planetary Science Letters*, *307*(1–2), 156–160. https://doi.org/10.1016/j.epsl.2011.04.026

Green, A., & Lane, R. (2003). Estimating noise levels in AEM data. *ASEG Extended Abstracts*, *2003*(2), 1–5. https://doi.org/10.1071/ASEG2003ab093

Guppy, L., Uyttendaele, P., Villholth, K. G., & Smakhtin, V. (2018). Groundwater and sustainable development Goals: Analysis of interlinkages. In *UNU-INWEH report series, issue 04*. United Nations University. Retrieved from https://hdl.handle.net/10568/98576

Hammond, W., Blewitt, G., Kreemer, C., & Nerem, S. (2021). GPS imaging of global vertical land motion for studies of sea level rise. *Journal of Geophysical Research: Solid Earth*, *126*(7), e2021JB022355. https://doi.org/10.1029/2021JB022355

Han, S. C., Sauber, J., Luthcke, S. B., Ji, C., & Pollitz, F. F. (2008). Implications of postseismic gravity change following the great 2004 Sumatra-Andaman earthquake from the regional harmonic analysis of GRACE intersatellite tracking data. *Journal of Geophysical Research*, *113*(B11), B11413. https://doi.org/10.1029/2008JB005705

Hartmann, A., Liu, Y., Olarinoye, T., Berthelin, R., & Marx, V. (2020). Integrating field work and large-scale modeling to improve assessment of karst water resources. *Hydrogeology Journal*, *29*(1), 315–329. https://doi.org/10.1007/s10040-020-02258-z

Hastings, D. (2014). *California's Central Valley: Producing America's fruits and vegetables*. House Natural Resources Committee Press. Retrieved from https://republicans-naturalresources.house.gov/uploadedfiles/2_5_14_ca_ri.pdf

Heggy, E., & Paillou, P. (2006). Probing structural elements of small buried craters using ground-penetrating radar in the southwestern Egyptian desert: Implications for Mars shallow sounding. *Geophysical Research Letters*, *33*(5), L05202. https://doi.org/10.1029/2005GL024263

Helm, D. C. (1975). One-dimensional simulation of aquifer system compaction near pixley, California: 1. Constant parameters. *Water Resources Research*, *11*(3), 465–478. https://doi.org/10.1029/wr011i003p00465

Hoffmann, J., Leake, S. A., Galloway, D. L., & Wilson, A. M. (2003). MODFLOW-2000 ground-water model – User guide to the subsidence and aquifer-system compaction (SUB) package Open-File Report 2003-233, 44. U.S. Geological Survey. Retrieved from http://pubs.usgs.gov/of/2003/ofr03-233/

Hooper, A., Zebker, H., Segall, P., & Kampes, B. (2004). A new method for measuring deformation on volcanoes and other natural terrains using InSAR persistent scatterers. *Geophysical Research Letters*, *31*(23). https://doi.org/10.1029/2004GL021737

Houborg, R., Rodell, M., Li, B., Reichle, R., & Zaitchik, B. F. (2012). Drought indicators based on model-assimilated Gravity Recovery and Climate Experiment (GRACE) terrestrial water storage observations. *Water Resources Research*, *48*(7). https://doi.org/10.1029/2011WR011291

Hwang, C., Yang, Y., Kao, R., Han, J., Shum, C. K., Galloway, D. L., et al. (2016). Time-varying land subsidence detected by radar altimetry: California, Taiwan and north China. *Scientific Reports*, *6*(1), 1–12. https://doi.org/10.1038/srep28160

Jackson, T. J. (2002). Remote sensing of soil moisture: Implications for groundwater recharge. *Hydrogeology Journal*, *10*(1), 40–51. https://doi.org/10.1007/s10040-001-0168-2

Jafari, F., Javadi, S., Golmohammadi, G., Karimi, N., & Mohammadi, K. (2016). Numerical simulation of groundwater flow and aquifer-system compaction using simulation and InSAR technique: Saveh basin, Iran. *Environmental Earth Sciences*, *75*(9), 833. https://doi.org/10.1007/s12665-016-5654-x

Jarvis, T., Giordano, M., Puri, S., Matsumoto, K., & Wolf, A. (2005). International borders, ground water flow, and hydroschizophrenia. *Groundwater*, *43*(5), 764–770. https://doi.org/10.1111/j.1745-6584.2005.00069.x

Kim, K. H., Liu, Z., Rodell, M., Beaudoing, H., Massoud, E., Kitchens, J., et al. (2021). An Evaluation of Remotely Sensed and In Situ Data Sufficiency for SGMA-Scale Groundwater Studies in the Central Valley, California. *JAWRA Journal of the American Water Resources Association*, *57*(5), 664–674.

Kirsch, R. (2006). Hydrogeophysical properties of permeable and low permeable rocks. In R. Kirsch (Ed.), *Groundwater geophysics – a tool for hydrogeology* (pp. 1–22). Springer.

Knight, R., Smith, R., Asch, T., Abraham, J., Cannia, J., Viezzoli, A., & Fogg, G. (2018). Mapping aquifer systems with airborne electromagnetics in the Central Valley of California. *Groundwater*, *56*(6), 893–908. https://doi.org/10.1111/gwat.12656

Kollet, S. J., & Maxwell, R. M. (2006). Integrated surface–groundwater flow modeling: A free-surface overland flow boundary condition in a parallel groundwater flow model. *Advances in Water Resources*, *29*(7), 945–958. https://doi.org/10.1016/j.advwatres.2005.08.006

Konikow, L. F. (2011). Contribution of global groundwater depletion since 1900 to sea-level rise. *Geophysical Research Letters*, *38*(17). https://doi.org/10.1029/2011GL048604

Kornfeld, R. P., Arnold, B. W., Gross, M. A., Dahya, N. T., Klipstein, W. M., Gath, P. F., & Bettadpur, S. (2019). GRACE-FO: The gravity recovery and climate experiment follow-on mission. *Journal of Spacecraft and Rockets*, *56*(3), 931–951. https://doi.org/10.2514/1.A34326

Kumar, M. D. (2005). Impact of electricity prices and volumetric water allocation on energy and groundwater demand management: Analysis from Western India. *Energy Policy*, *33*(1), 39–51. https://doi.org/10.1016/S0301-4215(03)00196-4

Kumar, S. V., Peters-Lidard, C. D., Tian, Y., Houser, P. R., Geiger, J., Olden, S., et al. (2006). Land information system: An interoperable framework for high resolution land surface modeling. *Environmental Modelling & Software*, *21*(10), 1402–1415. https://doi.org/10.1016/j.envsoft.2005.07.004

Kumar, S. V., Zaitchik, B. F., Peters-Lidard, C. D., Rodell, M., Reichle, R., Li, B., et al. (2016). Assimilation of gridded GRACE terrestrial water storage estimates in the North American land data assimilation system. *Journal of Hydrometeorology*, *17*(7), 1951–1972. https://doi.org/10.1175/JHM-D-15-0157.1

Kuo, C. Y., Cheng, Y. J., Lan, W. H., & Kao, H. C. (2015). Monitoring vertical land motions in southwestern Taiwan with retracked TOPEX/Poseidon and Jason-2 satellite altimetry. *Remote Sensing*, *7*(4), 3808–3825. https://doi.org/10.3390/rs70403808

Landerer, F. W., Flechtner, F. M., Save, H., Webb, F. H., Bandikova, T., Bertiger, W. I., et al. (2020). Extending the global mass change data record: GRACE follow-on instrument and science data performance. *Geophysical Research Letters*, *47*(12), e2020GL088306. https://doi.org/10.1029/2020GL088306

Landerer, F. W., & Swenson, S. C. (2012). Accuracy of scaled GRACE terrestrial water storage estimates. *Water Resources Research*, *48*(4). https://doi.org/10.1029/2011WR011453

Li, Z., Cao, Y., Wei, J., Duan, M., Wu, L., Hou, J., & Zhu, J. (2019). Time-series InSAR ground deformation monitoring: Atmospheric delay modeling and estimating. *Earth-Science Reviews*, *192*, 258–284. https://doi.org/10.1016/j.earscirev.2019.03.008

Li, Z., Fielding, E. J., Cross, P., & Preusker, R. (2009). Advanced InSAR atmospheric correction: MERIS/MODIS combination and stacked water vapour models. *International Journal of Remote Sensing*, *30*(13), 3343–3363. https://doi.org/10.1080/01431160802562172

Li, Z. W., Xu, W. B., Feng, G. C., Hu, J., Wang, C. C., Ding, X. L., & Zhu, J. J. (2012). Correcting atmospheric effects on InSAR with MERIS water vapour data and elevation-dependent interpolation model. *Geophysical Journal International*, *189*(2), 898–910. https://doi.org/10.1111/j.1365-246X.2012.05432.x

Liu, Z., Liu, P. W., Massoud, E., Farr, T. G., Lundgren, P., & Famiglietti, J. S. (2019). Monitoring groundwater change in California's Central Valley using sentinel-1 and GRACE observations. *Geosciences*, *9*(10), 436. https://doi.org/10.3390/geosciences9100436

Luthcke, S. B., Sabaka, T. J., Loomis, B. D., Arendt, A. A., McCarthy, J. J., & Camp, J. (2013). Antarctica, Greenland and Gulf of Alaska land-ice evolution from an iterated GRACE global mascon solution. *Journal of Glaciology*, *59*(216), 613–631. https://doi.org/10.3189/2013JoG12J147

Maxwell, R. M., Chow, F. K., & Kollet, S. J. (2007). The groundwater–land-surface–atmosphere connection: Soil moisture effects on the atmospheric boundary layer in fully-coupled simulations. *Advances in Water Resources*, *30*(12), 2447–2466. https://doi.org/10.1016/j.advwatres.2007.05.018

Maxwell, R. M., Condon, L. E., & Kollet, S. J. (2015). A high-resolution simulation of groundwater and surface water over most of the continental US with the integrated hydrologic model ParFlow v3. *Geoscientific Model Development*, *8*(3), 923–937. https://doi.org/10.5194/gmd-8-923-2015

Maxwell, R. M., & Kollet, S. J. (2008). Interdependence of groundwater dynamics and land-energy feedbacks under climate change. *Nature Geoscience*, *1*(10), 665–669. https://doi.org/10.1038/ngeo315

Maxwell, R. M., Lundquist, J. K., Mirocha, J. D., Smith, S. G., Woodward, C. S., & Tompson, A. F. (2011). Development of a coupled groundwater–atmosphere model. *Monthly Weather Review*, *139*(1), 96–116. https://doi.org/10.1175/2010MWR3392.1

McCallum, I., Montzka, C., Bayat, B., Kollet, S., Kolotii, A., Kussul, N., et al. (2020). Developing food, water and energy nexus workflows. *International Journal of Digital Earth*, *13*(2), 299–308. https://doi.org/10.1080/17538947.2019.1626921

Meinzer, O. E. (1932). *Outline of methods for estimating ground-water supplies (No. 638-C)*. USGPO. https://doi.org/10.3133/wsp638C

Meyer, F. J. (2011). Performance requirements for ionospheric correction of low-frequency SAR data. *IEEE Transactions on Geoscience and Remote Sensing*, *49*(10), 3694–3702. https://doi.org/10.1109/TGRS.2011.2146786

Michael, H. A., Post, V. E., Wilson, A. M., & Werner, A. D. (2017). Science, society, and the coastal groundwater squeeze. *Water Resources Research*, *53*(4), 2610–2617. https://doi.org/10.1002/2017WR020851

Milillo, P., Perissin, D., Salzer, J. T., Lundgren, P., Lacava, G., Milillo, G., & Serio, C. (2016). Monitoring dam structural health from space: Insights from novel InSAR techniques and multi-parametric modeling applied to the Pertusillo dam Basilicata, Italy. *International Journal of Applied Earth Observation and Geoinformation*, *52*, 221–229. https://doi.org/10.1016/j.jag.2016.06.013

Minsley, B. J. (2011). A trans-dimensional Bayesian Markov chain Monte Carlo algorithm for model assessment using frequency-domain electromagnetic data. *Geophysical Journal International*, *187*(1), 252–272. https://doi.org/10.1111/j.1365-246x.2011.05165.x

Minsley, B. J., Rigby, J. R., James, S. R., Burton, B. L., Knierim, K. J., Pace, M. D., et al. (2021). Airborne geophysical surveys of the lower Mississippi Valley demonstrate system-scale mapping of subsurface architecture. *Communications Earth and Environment*, *2*(1), 1–14. https://doi.org/10.1038/s43247-021-00200-z

Motagh, M., Shamshiri, R., Haghighi, M. H., Wetzel, H. U., Akbari, B., Nahavandchi, H., et al. (2017). Quantifying groundwater exploitation induced subsidence in the Rafsanjan plain, southeastern Iran, using InSAR time-series and in situ measurements. *Engineering Geology*, *218*, 134–151. https://doi.org/10.1016/j.enggeo.2017.01.011

Mukherjee, D., Heggy, E., & Khan, S. D. (2010). Geoelectrical constraints on radar probing of shallow water-saturated zones within karstified carbonates in semi-arid environments. *Journal of Applied Geophysics*, *70*(3), 181–191. https://doi.org/10.1016/j.jappgeo.2009.11.005

NASEM (National Academies of Sciences, Engineering, and Medicine). (2019). *Environmental engineering for the 21st Century: Addressing Grand challenges*. The National Academies Press. https://doi.org/10.17226/25121

NIC (National Intelligence Council). (2012). Global water security—Intelligence community assessment. Retrieved from https://www.dni.gov/files/documents/Special%20Report_ICA%20Global%20Water%20Security.pdf

O'Connell, Y., Brown, C., Henry, T., Morrison, L., & Daly, E. (2020). Quantitative assessment of groundwater resources using airborne electromagnetic remote sensing. *Journal of Applied Geophysics*, *175*, 103990. https://doi.org/10.1016/j.jappgeo.2020.103990

OECD (Organisation for Economic Co-operation and Development), Marchal, V., Dellink, R., Van Vuuren, D., Clapp, C., Chateau, J., & Van Vliet, J. (2011). OECD environmental outlook to 2050. *Organization for Economic Co-operation and Development*, *8*, 397–413. Retrieved from https://www.oecd.org/env/indicators-modelling-outlooks/49844953.pdf

Paine, J. G. (2003). Determining salinization extent, identifying salinity sources, and estimating chloride mass using surface, borehole, and airborne electromagnetic induction methods. *Water Resources Research*, *39*(3). https://doi.org/10.1029/2001wr000710

Paine, J. G., & Minty, R. S. (2005). Airborne hydrogeophysics. In Y. Rubin & S. S. Hubbard (Eds.), *Hydrogeophysics* (pp. 333–357). Springer.

Palacky, G. J. (1993). Use of airborne electromagnetic methods for resource mapping. *Advances in Space Research*, *13*(11), 5–14. https://doi.org/10.1016/0273-1177(93)90196-i

Pauloo, R. A., Fogg, G. E., Guo, Z., & Harter, T. (2020). Anthropogenic basin closure and groundwater salinization (ABCSAL). *Journal of Hydrology*, *593*, 125787. https://doi.org/10.1016/j.jhydrol.2020.125787

Peltier, W. R., Argus, D. F., & Drummond, R. (2018). Comment on the paper by Purcell et al. 2016 entitled 'An assessment of ICE-6G_C (VM5a) glacial isostatic adjustment model. *Journal of Geophysical Research: Solid Earth*, *122*(1), 450–487. https://doi.org/10.1002/2014jb011176

Poland, J. F., Ireland, R. L., Lofgren, B. E., & Pugh, R. G. (1975). Land subsidence in the san Joaquin Valley, California, as of 1972. Retrieved from https://pubs.usgs.gov/pp/0437h/report.pdf

Reager, J. T., Thomas, A. C., Sproles, E. A., Rodell, M., Beaudoing, H. K., Li, B., & Famiglietti, J. S. (2015). Assimilation of GRACE terrestrial water storage observations into a land surface model for the assessment of regional flood potential. *Remote Sensing*, *7*(11), 14663–14679. https://doi.org/10.3390/rs71114663

Reeves, J. A., Knight, R., Zebker, H. A., Kitanidis, P. K., & Schreüder, W. A. (2014). Estimating temporal changes in hydraulic head using InSAR data in the San Luis Valley, Colorado. *Water Resources Research*, *50*(5), 4459–4473. https://doi.org/10.1002/2013WR014938

Reeves, J. A., Knight, R., Zebker, H. A., Schreüder, W. A., Shanker Agram, P., & Lauknes, T. R. (2011). High quality InSAR data linked to seasonal change in hydraulic head for an agricultural area in the San Luis Valley, Colorado. *Water Resources Research*, *47*(12). https://doi.org/10.1029/2010WR010312

Richey, A. S., Thomas, B. F., Lo, M. H., Reager, J. T., Famiglietti, J. S., Voss, K., et al. (2015). Quantifying renewable groundwater stress with GRACE. *Water Resources Research*, *51*(7), 5217–5238. https://doi.org/10.1002/2015WR017349

Riley, F. S. (1969). Analysis of borehole extensometer data from central California. *International Association of Scientific hydrology*, *89*, 423–431.

Rodell, M., Chao, B. F., Au, A. Y., Kimball, J. S., & McDonald, K. C. (2005). Global biomass variation and its geodynamic effects: 1982–98. *Earth Interactions*, *9*(2), 1–19. https://doi.org/10.1175/EI126.1

Rodell, M., Chen, J., Kato, H., Famiglietti, J. S., Nigro, J., & Wilson, C. R. (2007). Estimating groundwater storage changes in the Mississippi River basin (USA) using GRACE. *Hydrogeology Journal*, *15*(1), 159–166. https://doi.org/10.1007/s10040-006-0103-7

Rodell, M., Famiglietti, J. S., Wiese, D. N., Reager, J. T., Beaudoing, H. K., Landerer, F. W., & Lo, M. H. (2018). Emerging trends in global freshwater availability. *Nature*, *557*(7707), 651–659. https://doi.org/10.1038/s41586-018-0123-1

Rodell, M., Houser, P. R., Jambor, U. E. A., Gottschalck, J., Mitchell, K., Meng, C. J., et al. (2004). The global land data assimilation system. *Bulletin of the American Meteorological Society*, *85*(3), 381–394. https://doi.org/10.1175/bams-85-3-381

Rodell, M., Velicogna, I., & Famiglietti, J. S. (2009). Satellite-based estimates of groundwater depletion in India. *Nature*, *460*(7258), 999–1002. https://doi.org/10.1038/nature08238

Rowlands, D. D., Luthcke, S. B., Klosko, S. M., Lemoine, F. G., Chinn, D. S., McCarthy, J. J., et al. (2005). Resolving mass flux at high spatial and temporal resolution using GRACE intersatellite measurements. *Geophysical Research Letters*, *32*(4). https://doi.org/10.1029/2004GL021908

Save, H., Bettadpur, S., & Tapley, B. D. (2016). High-resolution CSR GRACE RL05 mascons. *Journal of Geophysical Research: Solid Earth*, *121*(10), 7547–7569. https://doi.org/10.1002/2016JB013007

Scanlon, B. R., Longuevergne, L., & Long, D. (2012). Ground referencing GRACE satellite estimates of groundwater storage changes in the California Central Valley, USA. *Water Resources Research*, *48*(4). https://doi.org/10.1029/2011WR011312

Scibek, J., & Allen, D. M. (2006). Modeled impacts of predicted climate change on recharge and groundwater levels. *Water Resources Research*, *42*(11). https://doi.org/10.1029/2005WR004742

Scott, C. A., & Sharma, B. (2009). Energy supply and the expansion of groundwater irrigation in the Indus-Ganges Basin. *International Journal of River Basin Management*, *7*(2), 119–124. https://doi.org/10.1080/15715124.2009.9635374

Sengpiel, K. P., & Meiser, P. (1981). Locating the freshwater/salt water interface on the island of Spiekeroog by airborne EM resistivity/depth mapping. *Geologisches Jahrbuch C*, *29*, 255–271. http://www.swim-site.nl/pdf/swim06/swim_06-263-279.pdf

Sharma, K. D. (2009). Groundwater management for food security. *Current Science*, *96*(11), 1444–1447.

Sheridan, D. (1981). *Desertification of the United States*. Council on Environmental Quality.

Siemon, B., Christiansen, A. V., & Auken, E. (2009). A review of helicopter-borne electromagnetic methods for groundwater exploration. *Near Surface Geophysics*, *7*(5–6), 629–646. https://doi.org/10.3997/1873-0604.2009043

Siemon, B., van Baaren, E., Dabekaussen, W., Delsman, J., Dubelaar, W., Karaoulis, M., & Steuer, A. (2019). Automatic identification of fresh–saline groundwater interfaces from airborne electromagnetic data in Zeeland, The Netherlands. *Near Surface Geophysics*, *17*(1), 3–25. https://doi.org/10.1002/nsg.12028

Smith, B. D., Sengpiel, K. P., Plesha, J., & Horton, R. J. (1992). Airborne electromagnetic mapping of sub-surface brine, Brookhaven Oil Field, Mississippi. In *62nd SEG meeting* (pp. 340–343).

Smith, R., & Knight, R. (2019). Modeling land subsidence using InSAR and airborne electromagnetic data. *Water Resources Research*, *55*(4), 2801–2819. https://doi.org/10.1029/2018wr024185

Smith, R., & Li, J. (2021). Modeling elastic and inelastic pumping-induced deformation with incomplete water level records in Parowan Valley, Utah. *Journal of Hydrology*, *601*, 126654. https://doi.org/10.1016/j.jhydrol.2021.126654

Smith, R. G., Knight, R., Chen, J., Reeves, J. A., Zebker, H. A., Farr, T., & Liu, Z. (2017). Estimating the permanent loss of groundwater storage in the southern San Joaquin Valley, California. *Water Resources Research*, *53*(3), 2133–2148. https://doi.org/10.1002/2016wr019861

Smith, R. G., & Majumdar, S. (2020). Groundwater storage loss associated with land subsidence in Western United States mapped using machine learning. *Water Resources Research*, *56*(7), e2019WR026621. https://doi.org/10.1029/2019wr026621

Sneed, M. (2001). *Detection and measurement of land subsidence using global positioning system and interferometric synthetic aperture radar, Coachella Valley, California, 1996-98* (Vol. 1, No. 4193). US Department of the Interior, US Geological Survey. https://pubs.usgs.gov/wri/wri014193/wrir01-4193.pdf

Sneed, M., & Brandt, J. T. (2015). Land subsidence in the san Joaquin Valley, California, USA, 2007-2014. *Proceedings of the International Association of Hydrological Sciences*, *372*, 23–27. https://doi.org/10.5194/piahs-372-23-201

Spies, B., & Woodgate, P. (2003). Salinity mapping methods in the Australian context. Technical Report. *Programs Committee of the Natural Resource Management Ministerial Council and the National Dryland Salinity Program*.

Stokstad, E. (1999). Scarcity of rain, stream gages threatens forecasts. https://doi.org/10.1126/science.285.5431.1199

Swenson, S., & Wahr, J. (2002). Methods for inferring regional surface-mass anomalies from Gravity Recovery and Climate Experiment (GRACE) measurements of time-variable gravity. *Journal of Geophysical Research*, *107*(B9), ETG-3–ETG3-13. https://doi.org/10.1029/2001JB000576

Tapley, B. D., Bettadpur, S., Ries, J. C., Thompson, P. F., & Watkins, M. M. (2004). GRACE measurements of mass variability in the Earth system. *Science*, *305*(5683), 503–505. https://doi.org/10.1126/science.1099192

Terzaghi, K. (1925). Structure and volume of voids in soils, translated from Erdbaummechanik auf Bodenphysikalischer Grundlage. In *From theory to practice in soil mechanics*. John Wiley.

Upton, K. A., Butler, A. P., Jackson, C. R., & Mansour, M. (2019). Modelling boreholes in complex heterogeneous aquifers. *Environmental Modelling & Software*, *118*, 48–60. https://doi.org/10.1016/j.envsoft.2019.03.018

van Bussel, L. G., Grassini, P., Van Wart, J., Wolf, J., Claessens, L., Yang, H., et al. (2015). From field to atlas: Upscaling of location-specific yield gap estimates. *Field Crops Research*, *177*, 98–108. https://doi.org/10.1016/j.fcr.2015.03.005

Van Dijck, S. J., Laouina, A., Carvalho, A. V., Loos, S., Schipper, A. M., Van der Kwast, H., et al. (2006). Desertification in northern Morocco due to effects of climate change on groundwater recharge. In *Desertification in the mediterranean region. A security issue* (pp. 549–577). Springer. https://doi.org/10.1007/1-4020-3760-0_26

Vasco, D. W., Kim, K. H., Farr, T. G., Reager, J. T., Bekaert, D., Sangha, S. S., et al. (2022). Using Sentinel-1 and GRACE satellite data to monitor the hydrological variations within the Tulare Basin, California. *Nature Scientific Reports*, *12*(1), 3867. https://doi.org/10.1038/s41598-022-07650-1

Wada, Y., Van Beek, L. P., Van Kempen, C. M., Reckman, J. W., Vasak, S., & Bierkens, M. F. (2010). Global depletion of groundwater resources. *Geophysical Research Letters*, *37*(20). https://doi.org/10.1029/2010GL044571

Wahr, J., Molenaar, M., & Bryan, F. (1998). Time variability of the Earth's gravity field: Hydrological and oceanic effects and their possible detection using GRACE. *Journal of Geophysical Research*, *103*(B12), 30205–30229. https://doi.org/10.1029/98JB02844

Wang, J., Rothausen, S. G., Conway, D., Zhang, L., Xiong, W., Holman, I. P., & Li, Y. (2012). China's water–energy nexus: Greenhouse-gas emissions from groundwater use for agriculture. *Environmental Research Letters*, *7*(1), 014035. https://doi.org/10.1088/1748-9326/7/1/014035

Warner, N., Lgourna, Z., Bouchaou, L., Boutaleb, S., Tagma, T., Hsaissoune, M., & Vengosh, A. (2013). Integration of geochemical and isotopic tracers for elucidating water sources and salinization of shallow aquifers in the sub-Saharan Drâa Basin, Morocco. *Applied Geochemistry*, *34*, 140–151. https://doi.org/10.1016/j.apgeochem.2013.03.005

Watkins, M. M., Wiese, D. N., Yuan, D. N., Boening, C., & Landerer, F. W. (2015). Improved methods for observing Earth's time variable mass distribution with GRACE using spherical cap mascons. *Journal of Geophysical Research: Solid Earth*, *120*(4), 2648–2671. https://doi.org/10.1002/2014JB011547

Werner, A. D., & Simmons, C. T. (2009). Impact of sea-level rise on sea water intrusion in coastal aquifers. *Groundwater*, *47*(2), 197–204. https://doi.org/10.1111/j.1745-6584.2008.00535.x

White, A. M., Gardner, W. P., Borsa, A. A., Argus, D. F., & Martens, H. R. (2022). A review of GNSS/GPS in hydrogeodesy: Hydrologic loading applications and their implications for water resource research. *Water Resources Research*, *58*(7), e2022WR032078. https://doi.org/10.1029/2022wr032078

Wiese, D. N., Bienstock, B., Blackwood, C., Chrone, J., Loomis, B. D., Sauber-Rosenberg, J. M., et al. (2022). The mass change designated observable study: Overview and results. https://doi.org/10.1002/essoar.10510754.1

Wiese, D. N., Folkner, W. M., & Nerem, R. S. (2009). Alternative mission architectures for a gravity recovery satellite mission. *Journal of Geodesy*, *83*(6), 569–581. https://doi.org/10.1007/s00190-008-0274-1

Wiese, D. N., Nerem, R. S., & Han, S. C. (2011). Expected improvements in determining continental hydrology, ice mass variations, ocean bottom pressure signals, and earthquakes using two pairs of dedicated satellites for temporal gravity recovery. *Journal of Geophysical Research*, *116*(B11). https://doi.org/10.1029/2011JB008375

Wiese, D. N., Nerem, R. S., & Lemoine, F. G. (2012). Design considerations for a dedicated gravity recovery satellite mission consisting of two pairs of satellites. *Journal of Geodesy*, *86*(2), 81–98. https://doi.org/10.1007/s00190-011-0493-8

Wiese, D. N., Visser, P., & Nerem, R. S. (2011). Estimating low resolution gravity fields at short time intervals to reduce temporal aliasing errors. *Advances in Space Research*, *48*(6), 1094–1107. https://doi.org/10.1016/j.asr.2011.05.027

Wiese, D. N., Watkins, M. M., Yuan, D. N., Boening, C., & Landerer, F. W. (2016). The JPL RL05M GRACE mascon solution: Status, updates, and future prospects. *AGUFM*, G13A-1087.

Wolf, A. T. (2007). Shared waters: Conflict and cooperation. *Annual Review of Environment and Resources*, *32*(1), 241–269. https://doi.org/10.1146/annurev.energy.32.041006.101434

Wright, T. J., Parsons, B. E., & Lu, Z. (2004). Toward mapping surface deformation in three dimensions using InSAR. *Geophysical Research Letters*, *31*(1), L01607. https://doi.org/10.1029/2003GL018827

WWAP (United Nations World Water Assessment Programme). (2015). *The united nations world water development report 2015: Water for a sustainable world*. UNESCO. Retrieved from https://unesdoc.unesco.org/ark:/48223/pf0000231823_eng

Yang, X., Scuderi, L. A., Wang, X., Scuderi, L. J., Zhang, D., Li, H., et al. (2015). Groundwater sapping as the cause of irreversible desertification of Hunshandake Sandy Lands, Inner Mongolia, northern China. *Proceedings of the National Academy of Sciences*, *112*(3), 702–706. https://doi.org/10.1073/pnas.1418090112

Yeh, P. J. F., Swenson, S. C., Famiglietti, J. S., & Rodell, M. (2006). Remote sensing of groundwater storage changes in Illinois using the Gravity Recovery and Climate Experiment (GRACE). *Water Resources Research*, *42*(12). https://doi.org/10.1029/2006WR005374

Zaitchik, B. F., Rodell, M., & Reichle, R. H. (2008). Assimilation of GRACE terrestrial water storage data into a land surface model: Results for the Mississippi River basin. *Journal of Hydrometeorology*, *9*(3), 535–548. https://doi.org/10.1175/2007JHM951.1

Zebker, H. A., & Goldstein, R. M. (1986). Topographic mapping from interferometric synthetic aperture radar observations. *Journal of Geophysical Research*, *91*(B5), 4993–4999. https://doi.org/10.1029/JB091iB05p04993

Zeitoun, M., & Mirumachi, N. (2008). Transboundary water interaction I: Reconsidering conflict and cooperation. *International Environmental Agreements: Politics, Law and Economics*, *8*(4), 297–316. https://doi.org/10.1007/s10784-008-9083-5

Zektser, I. S., & Everett, L. G. (2004). *Groundwater resources of the world and their use*. United Nations Educational, Scientific and Cultural Organization.

Zhao, R., Li, Z. W., Feng, G. C., Wang, Q. J., & Hu, J. (2016). Monitoring surface deformation over permafrost with an improved SBAS-InSAR algorithm: With emphasis on climatic factors modeling. *Remote Sensing of Environment*, *184*, 276–287. https://doi.org/10.1016/j.rse.2016.07.019

Zhou, C., Gong, H., Chen, B., Zhu, F., Duan, G., Gao, M., & Lu, W. (2016). Land subsidence under different land use in the eastern Beijing plain, China 2005-2013 revealed by InSAR timeseries analysis. *GIScience and Remote Sensing*, *53*(6), 671–688. https://doi.org/10.1080/15481603.2016.1227297